AD NUMBER

AD483152

NEW LIMITATION CHANGE

TO

Approved for public release, distribution unlimited

FROM

Distribution authorized to U.S. Gov't. agencies and their contractors; Administrative/Operational Use; MAR 1966. Other requests shall be referred to Army Engineer Research and Development Laboratories, Fort Belvoir, VA 22060.

AUTHORITY

USAMERDC Notice, 24 May 1971

TYCO

TYCO LABORATORIES, INC., BEAR HILL, WALTHAM, MASSACHUSETTS 02154 TELEPHONE 617 899 1650

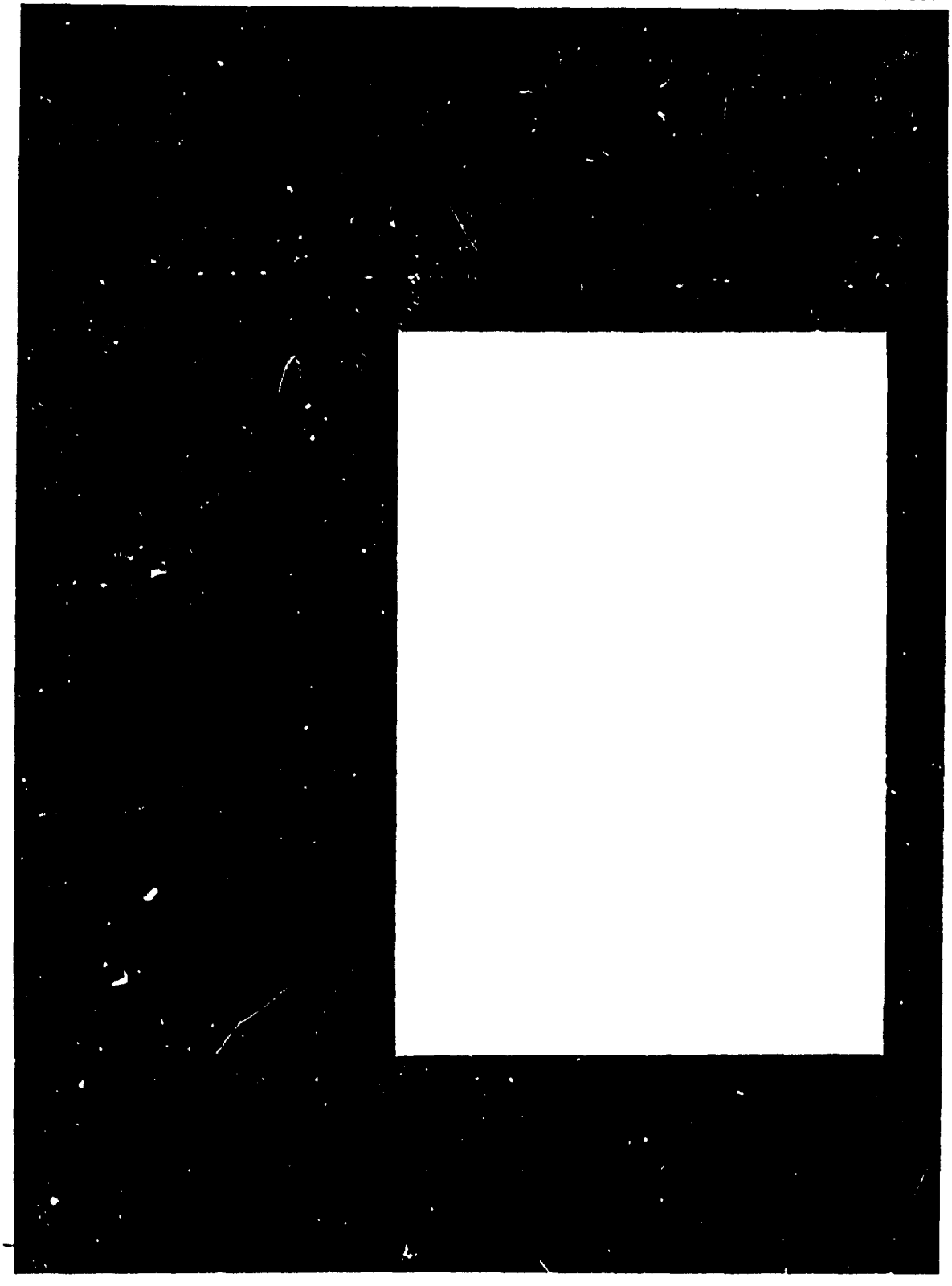

TYCO LABORATORIES, INC.
Bear Hill
Waltham, Massachusetts

Fifth Interim Technical Report

ELECTROCHEMICAL OXIDATION OF SATURATED HYDROCARBONS

covering period

November 1, 1965 through March 31, 1966

Contract No. DA 44-009-AMC-410(T)

Principal Investigators

S. B. Brummer and J. Giner

prepared for
U. S. Army Engineer Research and Development Laboratories
Fort Belvoir, Virginia

DDC AVAILABILITY NOTICE

Qualified requestors may obtain copies of this report from DDC.

CONTENTS

CONTENTS (Cont.)

LIST OF FIGURES

LIST OF FIGURES (Cont.)

LIST OF FIGURES (Cont.)

LIST OF TABLES

ABSTRACT

The aim of this work is to correlate the activity and stability of Pt-based catalysts for C_3H_8 electro-oxidation, with their structural properties. There are three distinct aspects to this study: (1) preparation of the catalyst, (2) its physical characterization, and (3) measurements of its catalytic activity.

Precipitation variables were selected during this period so as to map out conditions leading to high surface area materials. Nineteen Pt-blacks, prepared under various conditions by reduction of $PtCl_4$ or H_2PtCl_6 with formaldehyde in alkaline solution, had real surface areas varying between 3 and 48 m^2/g. The surface area depends on the concentration of the reactants, on the rate of alkalization, on the temperature, and on the presence or absence of oxygen in the solution. Mirror formation and colloidal dispersion are two phenomena repeatedly found and to some extent controlled during this period.

Electron microscopic shadowgraphy and selected area electron diffraction, X-ray diffraction, and BET showed that in some preparations all the elementary particles are single crystals, while in others they are polycrystalline. Shadowgraphy also provided valuable information on the structure (internal porosity) of the agglomerates.

Detailed X-ray diffraction studies show that the stored energy from stacking faults and twinning varies substantially for the three Pt-blacks studied. This X-ray method has been completely developed and can now be used routinely.

Techniques for preparing reproducible, Teflon-bonded micro-electrodes have been developed for testing the activity of Pt-black towards C_3H_8 oxidation. A "floating electrode" cell for half-cell studies has also been assembled. Tests with microelectrodes made from commercial Pt-black show that the procedures for electrode fabrication and test give highly reproducible results.

The corrosion of a number of metals, intermetallic compounds and alloys in hot, concentrated H_3PO_4 has been studied with the potentiostatic step technique. The metals Al, Ag, Co, Pb, Mo and Ni corrode very fast even at temperatures of only 80°C and cannot therefore be considered as possibilities for the major constituents of structural alloys. Cr corrodes slowly enough, even at 150°C, to show promise as an economically attractive alternative to Ta-based materials. However, thus far, intermetallic compounds based on Cr (e.g. Cr_2Ta, Cr_3Si, $CrSi_2$, Cr_3C_2) have been found to corrode more rapidly than Cr itself at elevated temperatures. The good corrosion resistance at elevated temperatures of a number of Ta compounds (TaNi, $TaNi_3$) and alloys (Ta-Ti) has been confirmed, but the resistance of other such compounds is surprisingly poor (e.g. $TaCo_3$). Possible reasons for this variation in behavior are discussed.

PART 1

I. ABSTRACT

The aim of this work is to correlate the activity and stability of Pt-based catalysts for C_3H_8 electro-oxidation, with their structural properties. There are three distinct aspects to this study: (1) preparation of the catalyst, (2) its physical characterization, and (3) measurements of its catalytic activity.

Precipitation variables were selected during this period so as to map out conditions leading to high surface area materials. Nineteen Pt-blacks, prepared under various conditions by reduction of $PtCl_4$ or H_2PtCl_6 with formaldehyde in alkaline solution, had real surface areas varying between 3 and 48 m^2/g. The surface area depends on the concentration of the reactants, on the rate of alkalization, on the temperature, and on the presence or absence of oxygen in the solution. Mirror formation and colloidal dispersion are two phenomena repeatedly found and to some extent controlled during this period.

Electron microscopic shadowgraphy and selected area electron diffraction, X-ray diffraction, and BET showed that in some preparations all the elementary particles are single crystals, while in others they are polycrystalline. Shadowgraphy also provided valuable information on the structure (internal porosity) of the agglomerates.

Detailed X-ray diffraction studies show that the stored energy from stacking faults and twinning varies substantially for the three Pt-blacks studied. This X-ray method has been completely developed and can now be used routinely.

Techniques for preparing reproducible, Teflon-bonded microelectrodes have been developed for testing the activity of Pt-black towards C_3H_8 oxidation. A "floating electrode" cell for half-cell studies has also been assembled. Tests with microelectrodes made from commercial Pt-black show that the procedures for electrode fabrication and test give highly reproducible results.

II. INTRODUCTION

The aim of this work is to correlate the activity and stability of Pt-based catalysts for C_3H_8 electro-oxidation with their structural properties. The structural properties include those pertaining to the elementary particles, such as composition (average) particle size and size distribution, concentration of defects (stored energy), morphology, etc., and those depending on the state of agglomeration, such as agglomerate size, internal pore distribution, apparent density, etc.

There are three distinct aspects to this work: (1) preparation of the catalyst, (2) physical characterization and (3) measurement of its catalytic activity. As information is gathered on these three aspects, correlations will be established between preparation conditions and structural factors, and between these and catalytic activity; in this way, we will be able to prepare reproducibly catalysts of controlled activity and stability.

Pure Pt-black catalysts are studied in the initial phase of the program. The preparation of platinum black deserves special study since the existing information is very limited (at least in the recent literature) and has a weak scientific basis. In addition, some of the observations reported in the older literature must be reinterpreted, using new concepts not available at that time.

After sufficient information is obtained on the conditions determining the preparation of Pt-black of maximum activity, we will concentrate on the study of co-precipitated and/or supported Pt-type catalysts.

III. SURVEY OF LITERATURE ON THE PREPARATION OF Pt-BLACK CATALYSTS

A. Introduction

Platinum black has been produced and studied for the past century and a half. However, the methods of production and the resulting material vary greatly; most of the literature is at least thirty years old. A good portion of the references quoted in this section were taken from Gmelin.

The recent literature concerning Pt-black describes the properties with regard to a specific use (such as in the application as fuel cell electrodes) without describing the preparation methods. In a few reports fast screening of preparation methods has been described without deeper study of the parameters concerning a given method.

The techniques for the preparation of platinum black are very numerous; however, one of the most widely studied reactions for the formation of a platinum black concerns the reduction of a platinum compound (usually $PtCl_4$ or H_2PtCl_6) with formaldehyde, formic acid, or sodium formate in a basic medium.

In addition, other methods using such reducing agents as H_2, N_2H_4, and citric acid have been described. Methods based on the reduction with borohydrides deserve separate studies since the final product is not necessarily pure Pt, but a mixture of Pt with dissolved boron and platinum boride[1, 2].

1. Preparation of Platinum Blacks by Reduction with Formaldehyde: A procedure for the reduction of platinic chloride with formaldehyde was given by Loew[3]. A platinic chloride solution is cooled and reacted with a 40 to 45% formaldehyde solution in a basic NaOH medium. After standing 12 hours, the precipitate is washed until the material starts to form a colloidal solution. Complete removal of the NaCl by washing is only possible after the wet platinum black has adsorbed oxygen under exothermic conditions and has been converted to a loose, porous mass. Unremoved NaCl will lower the catalytic activity of the black.

Willstätter and Waldschmidt-Leitz[4] considered some improvements suggested by Willstätter and Hatt[5] and modified Loew's original work to yield the following preparation: Eighty cubic centimeters of a solution of $H_2[PtCl_6]$ containing 20 grams of platinum and some free HCl are mixed with 150 cubic centimeters of a 33% solution of formaldehyde. After cooling to -10°C, the solution is reacted drop wise with 420 grams of a 50% KOH solution. During the procedure the temperature of the reaction mixture is not allowed to rise above 4° to 6°C. The two reacting solutions are completely mixed and the mixture is heated to 55° - 60°C with vigorous stirring for half an hour to deposit the platinum black. The black is washed first in a high cylinder by decantation until the reaction of alkali or Cl^- disappears and then on a suction filter using a slow filtration so that the material is always covered with water. At this point the substance is pressed rapidly between two filter papers and dried in a vacuum dessicator. Carbon dioxide is allowed to enter as the dessicator is opened. A similar preparation is discussed by Neuman and Goebel[6].

Sieverts and Brüning[7] reported that the reduction of $H_2[PtCl_6]$ is accelerated by using increasing amounts of formaldehyde and alkali. After cooling (and in an excess of alkali), 2 moles of formaldehyde are necessary to reduce 1 mole of $H_2[PtCl_6]$, the formaldehyde being oxidized to formate. When 1 mole of formaldehyde is used for 1 mole of $H_2[PtCl_6]$, the reduction will go to completion only after prolonged heating at 100°C where the formaldehyde oxidizes to carbonate. As a consequence of side reactions, it is not possible to follow the course of the reaction stoichiometry.

2. Preparation of Platinum Blacks by Reduction with Formic Acid or Alkali Formate: Dobereiner[8] reported on the preparation of platinum black by mixing a solution of 1 mole of $H_2[PtCl_6]$ with 2 moles of Na_2CO_3 and 1 mole of formic acid and thus warming the mixture. He also studied the formation of platinum black by reduction of $Na_2[PtCl_6]$ with formic acid[9, 10].

Gladstone and Tribe[11] worked on the reduction of a platinum salt with alkali formate. Along the same lines, Benton[12] prepared a platinum

black by pouring a hot 6% solution of $H_2[PtCl_6]$, which was neutralized with Na_2CO_3, slowly into the same volume of a boiling 5% solution of sodium formate. The resulting product is washed with hot water until the test for Cl^- is negative. Similar preparations were noted by Mond, Ramsay and Shields[13, 14], Gutbier and Maisch[15]; Graf[16]; and Wassiljew[17].

According to Sieverts and Brüning[18], the theoretical amount of sodium formate should be used to precipitate the platinum black. A solution of 12.81 g of $H_2[PtCl_6]$ (39 weight percent platinum) is added drop wise to a boiling solution of 3.5 grams of sodium formate and 8.2 grams of Na_2CO_3 in 100 cubic centimeters of water. After washing by frequent decantation with hot distilled water, most of the water is removed from the material in a glass filtering crucible. The final drying is done in a vacuum dessicator above pure, solid KOH. The amounts of carbonate and formate necessary to precipitate the platinum black should be at least the amounts given by the equation:

$$H_2[PtCl_6] + 2\,HCO_2Na + 2\,Na_2CO_3 = Pt + 6\,NaCl + 4\,CO_2 + 2\,H_2O.$$

If the amount of carbonate is not sufficient, platinum will be precipitated partially as a mirror. A black obtained in the presence of an excess of sodium formate always contains adsorbed formate which cannot be washed away; the formate can be removed as CO and H_2 by heating in a stream of CO_2. When heated in air, the adsorbed formate is oxidized and then the platinum itself is oxidized. Further heating of the oxidized platinum black in the absence of oxygen causes oxygen to be evolved. Using less than 2 moles of sodium formate for 1 mole of $H_2[PtCl_6]$, a black that contains platinum hydroxides is obtained and will evolve oxygen when heated. A black that does not evolve any gases when heated is obtained by using exactly 2 moles of sodium formate for 1 mole of $H_2[PtCl_6]$. The material obtained under these conditions is dark gray and is not so finely divided as that precipitated with excess of formate[7].

Schulze[19], as well as Wassiljew[17], reported that platinum blacks obtained by reduction with formic acid or formaldehyde have a tendency to form colloidal solutions, for example during the washing process.

3. Effect of Adsorbed Oxygen: Döbereiner[20-22] came to the conclusion that platinum black consists of finely divided platinum and adsorbed oxygen. Wöhler[23, 24] commented on the oxygen content of blacks precipitated with formaldehyde. According to Mond, Ramsay, and Shields[13, 14] platinum black obtained with sodium formate and dried at 100°C contains about 0.66 weight % (about 100 times its volume) of oxygen. Guthier and Maisch[15] set the figure at 0.55 weight %, as an average. Willstätter and Jaquet[25] found that material produced by formaldehyde reduction contains O and H, which cannot be removed completely even after drying for days above P_2O_5 in high vacuum. In subsequent storage under CO_2, water vapor is formed.

When adding calculated amounts of H_2, only a part of this gas reacts with adsorbed O_2 of the black while the rest of the H_2 is adsorbed as such. This observation was reported by Mond, Ramsay, and Shields[26, 27]. According to Willstätter and Waldschmidt-Leitz[4], platinum black can be obtained free of oxygen by prolonged action of H_2 on the material suspended in glacial acetic acid. They also found that an almost O_2-free black is obtained by keeping the black under a high vacuum for an extremely long period[4].

Döbereiner[21] recognized the importance of the O-content in the platinum black on its catalytic activity; a "black" prepared by reduction with formic acid becomes inactive but can be reactivated by taking up more oxygen. Euber[28], Wöhler[24], and Willstätter and Waldschmidt[4] reported about the indispensability of oxygen for the activity of platinum black.

The products which were deactivated and freed from oxygen by reduction or evacuation were found by Euler[28] to be dark gray, flocculent and sometimes of a crystalline aspect, as opposed to the deep black, fine powdery material which contained oxygen. In one case, Willstätter and Waldschmidt-Leitz[4] observed the formation of a large granular substance. The effect of chemisorbed oxygen in maintaining the activity of Pt black can be explained, at least in part, by the retarding action, observed recently by McKee[29], of chemisorbed oxygen on the low temperature sintering of Pt-

black. More difficult to explain is the reverse process, i.e. the reactivation of inactive Pt-black by action of oxygen; this point certainly deserves to be confirmed.

Wöhler[23], and Wöhler and Engler[30] found that in dilute HCl solution some of the active ("oxygenated") platinum black is transformed to a granular, fast sedimenting, inactive form and the rest of the black (10 to 18% when the original black is a very finely divided and thoroughly "oxidized" material) goes into solution. The same granular form is formed by the action of reducing agents, and, in this form, platinum is completely insoluble in HCl solution. When exposed to air, this inactive form is transformed easily to the active form, which is partially soluble in HCl. Wöhler[23] concluded from the solubility in HCl-solutions and from the close similarity of the chemical properties of the Pt(II)-oxyhydrate and platinum black that a very large part of the oxygen existing on the Pt-black is bound as the Pt(II)-oxyhydrate. Further discussion along these lines can be found in the work by Voorhees and Adams[31], and Kobosew and Anachin[32]. Willstätter and Waldschmidt-Leitz[4] discussed the way in which O and H can exist in platinum black. Breiter and Weininger[33] have shown recently in another connection that dissolution of "oxidized" Pt in HCl does not require the presence of bulk oxides or hydroxides. Platinum can be dissolved according to the anodic reaction of mixed electrode mechanisms with chemisorbed oxygen supplying the necessary cathodic current. This mechanism can explain easily the solubility of the active (oxygenated) Pt. The change in morphology (size increase) could be explained as a recrystallization phenomenon because under the present conditions, i.e. in the system: $Pt/PtCl_6^{=}$, Cl^-, H^+, a high rate for recrystallization at open circuit can be expected. Again, it is more difficult to explain the reverse phenomenon of reactivation of the inactive (reduced) Pt-black in the presence of oxygen.

4. Modifications of Highly Divided Pt-black: According to Gutbier and Maisch[15] and Gutbier and Neundlinger[34], platinum black exists as two modifications: (1) as a deep black, catalytically active substance and (2) as a gray black, less active substance which is considered

an intermediate stage between platinum black and platinum sponge. The gray black modification is obtained when platinum is precipitated from alkaline solution with sodium formate and the resulting material is treated with HCl or boiling water for a long while. The black modification is supposed to be restored by treating the gray black material with alkali. A solution of hydrazonium hydroxide gives the best results.

Under heat treatment platinum black is converted to platinum sponge with the evolution of O_2, H_2, CO_2 and CO, as reported by Sieverts and Brüning[7].

The differences between black and gray materials could be explained in terms of changes in real surface area. However, since it is possible to obtain "gray" materials (as will be shown when describing the results) with higher surface areas than many "black" materials, this simple explanation is not sufficient.

5. Carbon Containing Impurities: Platinum black is found to contain carbon when prepared by reduction with organic compounds. This fact was reported by Döbereiner[35].

Sieverts and Brüning[7] found that platinum black obtained by reduction with formate or formaldehyde contains several impurities composed of C, O, and H, depending on the preparation conditions. The impurities cannot be removed without destruction of the state of fine division of the black. This phenomenon was also reported by Mond, Ramsay, and Shields[14].

In view of the results obtained from studies of the anodic oxidation of hydrocarbon compounds (see for instance references 36-38), these impurities can now be regarded as chemisorbed intermediates of formaldehyde or formic acid oxidation.

6. Mirror Formation: A frequent and undesired phenomenon is the reduction of Pt to mirrors floating on the free reaction surface or attached to the walls of the reaction vessel. Sieverts and Brüning[7] discuss the effect of reactant concentrations on the formation of mirrors during the preparation of platinum black by reduction with formaldehyde and with

formate. It has been suggested that mirror formation indicates reduced catalytic activity of the simultaneously deposited black. The mechanisms of mirror formation deserve some investigation.

7. Colloidal Solutions: The often observed tendency of platinum black to form colloidal solutions when washed with water is related by Wassiljew[17] to the presence of portions of the platinum black which contain oxygen.

Suggestions to avoid the formation of colloidal platinum, expecially from the material formed according to the procedure of Loew[3], are numerous. Houben and Pfau[39] heated the reaction mixture for one hour on a water bath. Courtot[40] weakly acidified the reaction mixture with HCl. Feulgen[41] suggested that the reaction mixture be warmed at 55°C for one half hour and afterwards be vigorously shaken and acidified weakly with acetic acid. Taylor, Kistiakowsky, and Perry[42] proposed pouring the solution of $PtCl_4$ and formaldehyde into a boiling solution of NaOH. Boswell and McLaughlin[43] stated that the solution of $PtCl_4$, HCOOH, and NaOH should be allowed to stand for 48 hours at temperatures not exceeding 10°C prior to filtration. Resins are formed above 10°C (probably by polymerization of the aldehyde) which act as a protective colloid.

8. Storage: Courtot[40] discovered that platinum black retains its activity after one year if it is kept above H_2SO_4 in a closed dessicator.

Houben and Pfau[39] found that the activity remains practically unchanged when the black is stored in distilled water in a sealed flask which is as free as possible from air.

B. Experimental Results

1. Model of Platinum Precipitations: Reduction of H_2PtCl_6 or $PtCl_4$ with formaldehyde was selected initially for obtaining Pt-black of varying physical properties because, as shown above, it is the best known process and also because it is a relatively easy process to study from the point of view of the mixed electrode model. According to this model, discussed in detail in the Fourth Interim Report, the initial nucleation process

is followed by an electrochemical deposition of Pt coupled with an anodic oxidation of the reducing agent. Although both electrode processes occur on the nucleus simultaneously and at the same rate, they are essentially independent of each other. Under these conditions the reactivity, concentration, etc., of the reducing agent determines the rate of electrodeposition of Pt and the electrical potential of the growing particles. The rate of electrodeposition determines in turn the morphology of the electrode deposit in much the same fashion as external current determines the structure of deposits plated on macroscopic electrodes.

No reaction occurs after mixing H_2PtCl_6 with formaldehyde, as long as the solution is acid, even if the solution is boiled. This behavior can be interpreted using the experiment of Fig. 1.1 based on the mixed electrode model; Curve a of Fig. 1.1 is the i(E)-curve for electrodeposition of H_2PtCl_6 in absence of HCHO in acid and curve b is the i(E)-curve for the oxidation of HCHO in absence of H_2PtCl_6, also in acid. Since the oxidation of formaldehyde occurs at potentials higher than the reduction potential of platinum, a reduction of Pt cannot occur. In base, on the contrary, (Fig. 1.2) the potential of oxidation of formaldehyde is more negative than that of $PtCl_6^=$ reduction (both because of thermodynamic and kinetic reasons); as a consequence, $PtCl_6^=$ reduction is possible. Once the nuclei are formed, the growing particles will establish that potential at which the current for oxidation of formaldehyde becomes equal to the current for reduction of $PtCl_6^=$. Since the diffusion conditions are not the same and since some specific interaction of the partial reactions is probable, the actual potential of the growing particles will be quantitatively different from the potential deduced from i(E)-curves obtained on Pt immersed in separate solution of reactants at the same (bulk) concentration. It should also be noticed that although theoretically the particle potential and the rate of Pt deposition (and therefore the particle structure) can be controlled by selecting the concentrations, this selection is limited, in practice, by the change of reactant concentration (especially of $PtCl_6^=$) during the course of reaction. Therefore, if the particle properties are a function of the concentration of the reactants (as expected), it is likely that the properties of the particle will change in the course of precipitation.

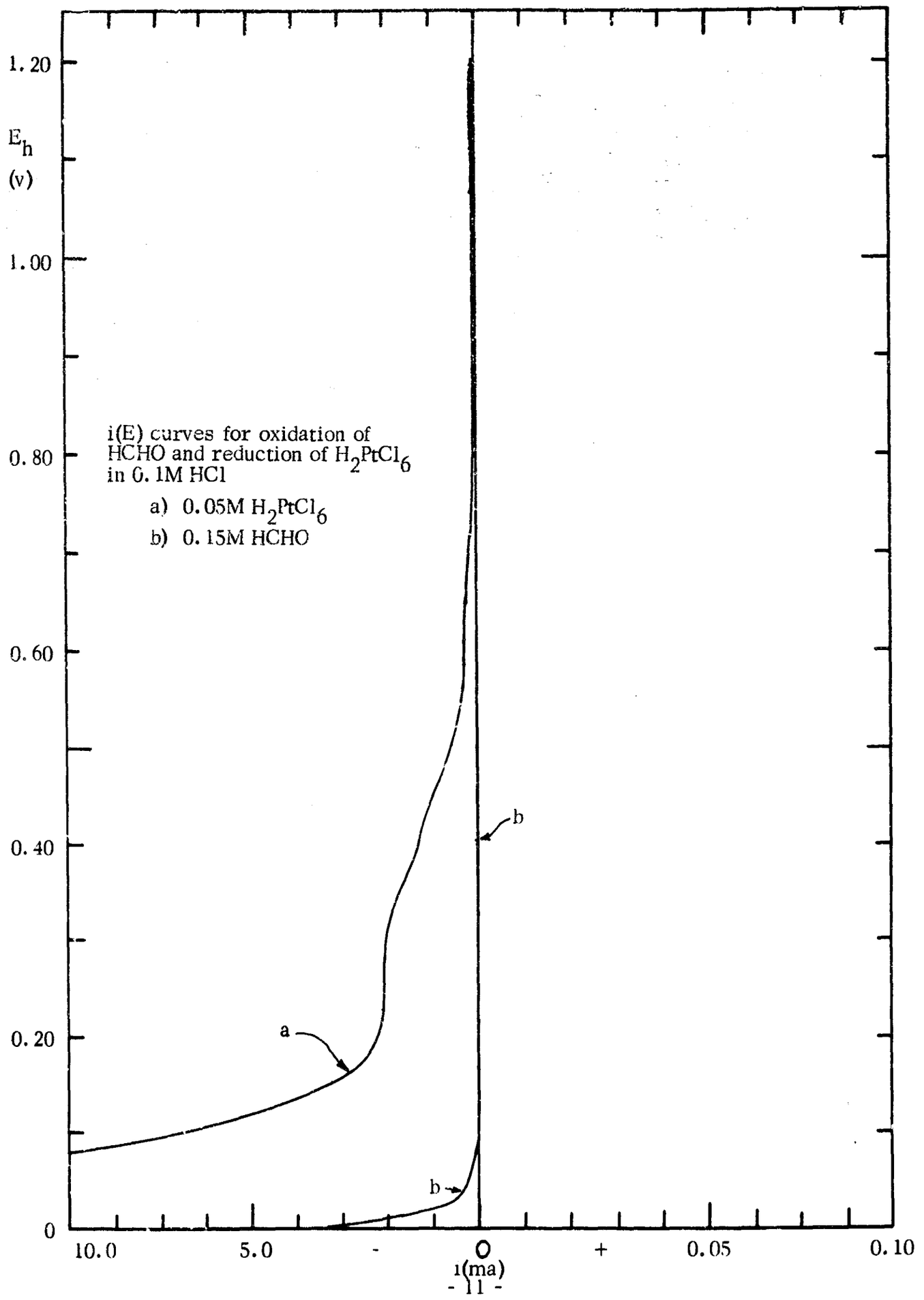
1.20
E_h
(v)
1.00
0.80
0.60
0.40
0.20
0
i(E) curves for oxidation of
HCHO and reduction of H_2PtCl_6
in 0.1M HCl
a) 0.05M H_2PtCl_6
b) 0.15M HCHO
a
b
b
10.0
5.0
-
0
+
0.05
0.10
i(ma)

Fig. 1.2

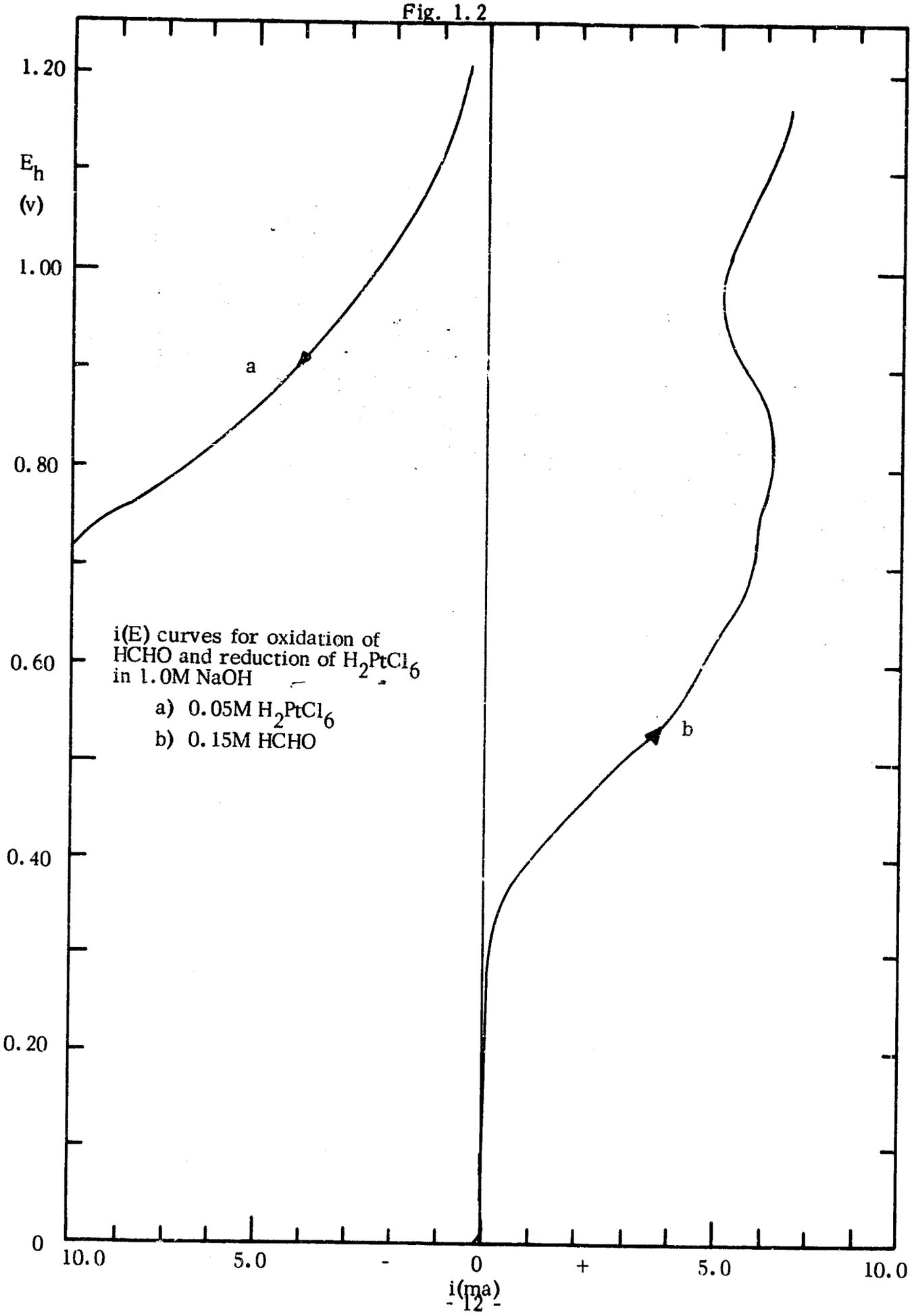
1.20
E_h
(v)
1.00
0.80
0.60
0.40
0.20
0
a
b
i(E) curves for oxidation of HCHO and reduction of H_2PtCl_6 in 1.0M NaOH
a) 0.05M H_2PtCl_6
b) 0.15M HCHO
10.0
5.0
-
0
+
5.0
10.0
i(ma)

In order to check the model of the mixed electrode, the potential of a Pt microelectrode was measured during the course of the reaction starting with acid solutions of H_2PtCl_6 and HCHO and adding NaOH in order to cause the reaction to proceed.

To measure this potential, as well as pH variation during the reaction, a three electrode system was used in conjunction with a Leeds and Northrup pH-meter-voltmeter. The pH of the solution was measured as a function of time with a glass electrode; the mixed electrode potential was measured with a platinum microelectrode. In both cases a calomel electrode was used as the reference. A one rpm motor was fitted with a notched cam which activated a micro-switch every 15 seconds switching between the glass electrode and the platinum electrode. Thus, the pH and the potential of the Pt microelectrode were recorded alternatingly. All the potentials were corrected to the reversible H_2-electrode at the pH considered.

Fig. 1.3 shows a typical curve obtained for this system. After alkalization, the microelectrode remains for thirty minutes at a high potential of $E_h > 700$ mv and then very quickly decreases to 200 mv. Corresponding closely to this abrupt change of potential, there is a darkening of the solution due to Pt black precipitation. This darkening is quantitatively shown in Fig. 1.4, where the variation of optical density, as followed with a colorimeter, is recorded together with the pH and mixed potential. It can be suggested that the time at high potential corresponds to an induction period during which nuclei are formed. The formation of nuclei is not as yet well understood; they may be induced by particles of extraneous material or even by the Pt-microelectrode, if one is used. In this respect, it is interesting to note that during precipitation without stirring (sample 73-23), a mirror was formed on the free surface of the solution and platinum black was formed immediately below the surface. The platinum black layer grew from the surface into the solution until a thickness of 4 cm, or two thirds the depth of the reaction vessel, was reached. Afterwards, due to convection, the black was homogeneously distributed through the solution. In this case, the nucleus is apparently the two dimensional layer of the mirror from which a dendritic type of growth progesses into solution. The

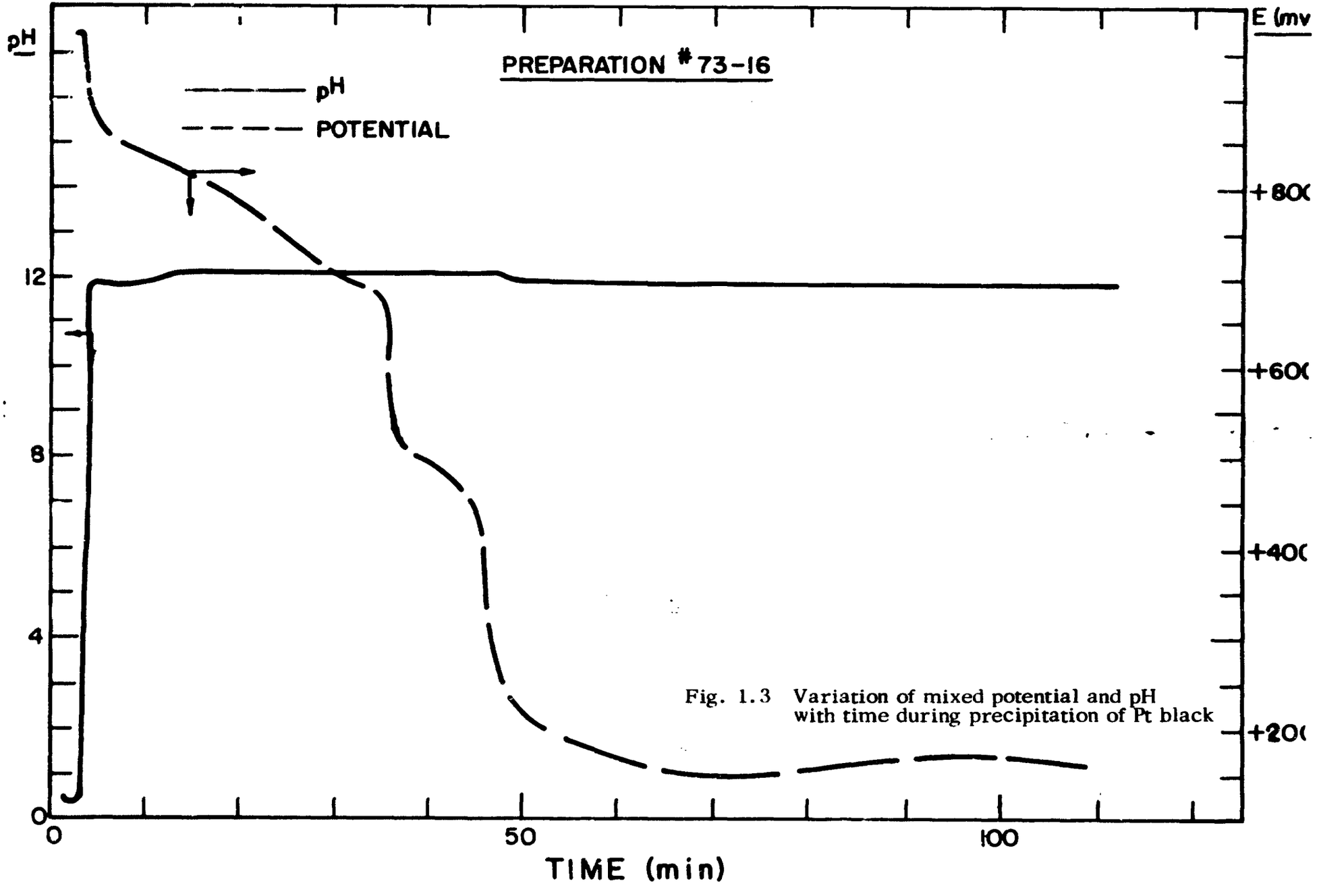

Fig. 1.3 Variation of mixed potential and pH with time during precipitation of Pt black

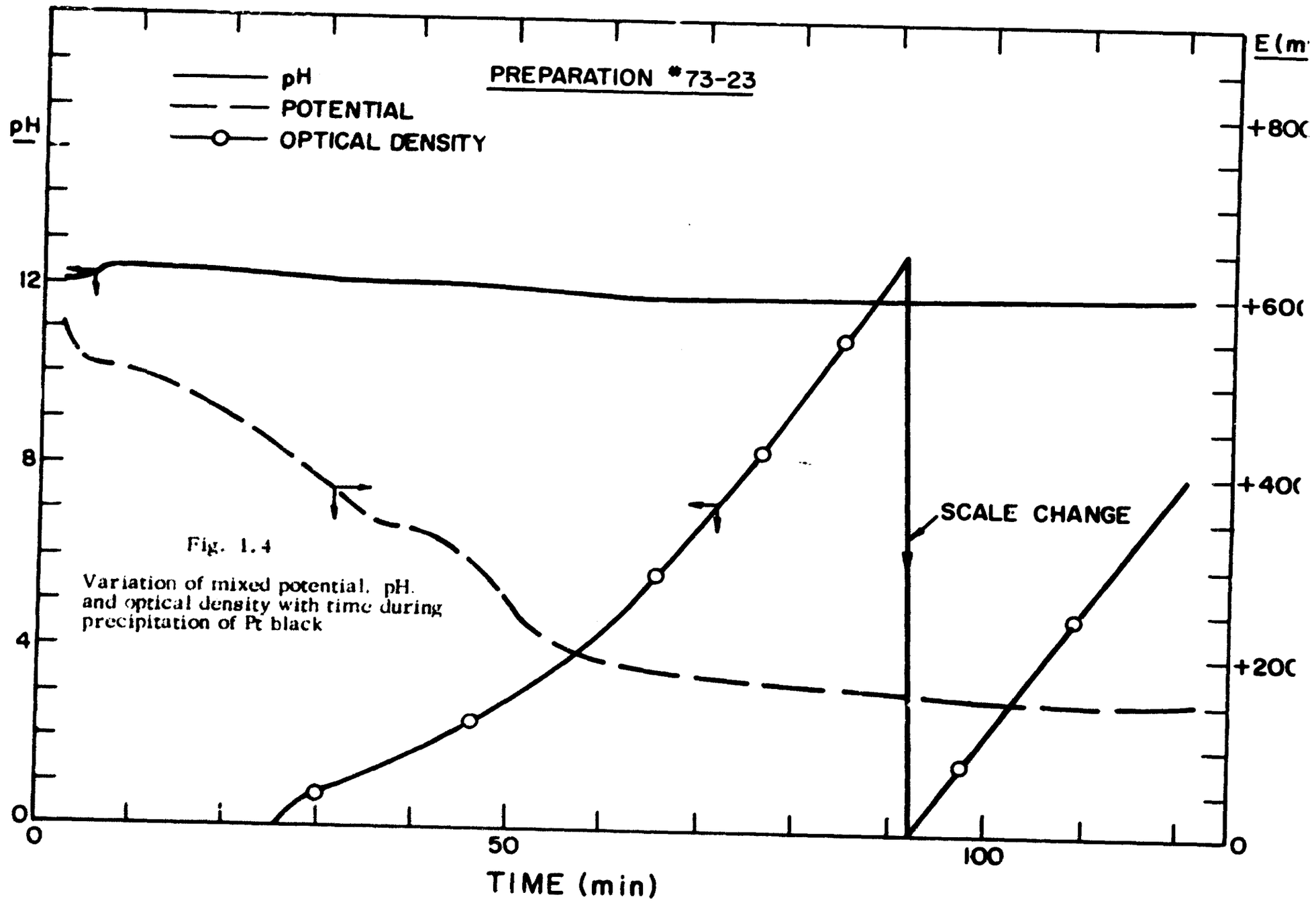

Fig. 1.4

Variation of mixed potential, pH, and optical density with time during precipitation of Pt black

reason for the formation or accumulation of nuclei on the free surface is not yet known. From Fig. 1.3 we also conclude that precipitation occurs always at sufficiently positive potentials to eliminate any chance of H_2-evolution during precipitation.

2. Selection of Precipitation Conditions: In order to obtain Pt black with different physical properties, the following conditions have been varied in the preparations:

a) Concentration of the Pt salt (H_2PtCl_6 in all but six cases) and concentration of the formaldehyde. Basically, four conditions are of interest: (1) high concentrations of both reactants; (2) low concentrations of both reactants, (3) high concentration of H_2PtCl_6 and low concentration of HCHO, and (4) low concentration of H_2PtCl_6 and high concentration of HCHO. As mentioned above, the initial conditions change during the course of the reaction. The obvious procedure of interrupting the reaction (e.g., by acidification), when only a fraction of the reactants, especially H_2PtCl_6, have been consumed, is impractical for preparation of sizable amounts of catalysts; in addition, considerable recrystallization could occur on a Pt black in the presence of unreacted H_2PtCl_6. These difficulties also make impractical the reaction of a solution which is very concentrated in H_2PtCl_6 and very dilute with respect to HCHO, unless HCHO is added continuously. Constant addition of HCHO may cause high localized concentrations of this reactant.

b) pH of reaction or, what is similar, rate of alkalization. The two extreme cases are the addition of concentrated alkali solution all at once and the addition of diluted alkali slowly. The reaction will be much faster in the first case than in the second case.

c) Temperature. Low temperatures are recommended in the literature. Low temperatures may decrease the rate of surface diffusion of Pt ad-atoms during precipitation. A decrease of temperature also increases the viscosity of the solutions. A low temperature (0-10°C) is not necessary for obtaining a finely divided precipitate of Pt black. As will be seen later, Pt blacks with high surface areas can be obtained even if the temperature is 100°C during precipitation.

d) In addition to the above, secondary conditions can be changed; for example, oxygen can be bubbled through the solution after precipitation. Some of these conditions cause a change in the Galvani potential of the colloidal particles and, therefore, in the ζ-potential which regulates their repulsion.

3. Description of the Preparations: The catalysts prepared are described below and in Table 1.1. In general, the chloroplatinic acid (or platinum tetrachloride) and formaldehyde solutions were first mixed and then a NaOH solution was added to precipitate platinum black. Concentration of H_2PtCl_6 and HCHO are computed on the basis of the total volume of solution, including the volume of the added NaOH. In some cases, NaOH was added slowly (dropwise); in these, the concentrations of H_2PtCl_6 and HCHO refer to the original solution and do not include the dilution produced by addition of NaOH.

Normally, the reaction mixture was stirred until platinum black began to precipitate. Stirring was discontinued at this point to avoid coagulation of the particles (see #73-12 in Table 1.1 for effect of stirring after precipitation).

In two cases (73-11, 73-19), the NaOH and H_2PtCl_6 solutions were mixed first and then HCHO added. The order of mixing does not appear to have any significant effect on the course of the reaction.

a) Platinum Black #73-10. Seven grams of $PtCl_4$ were dissolved in 50 ml of water and 15 ml of a 37% HCHO solution. The mixture was cooled in a dry ice-isopropyl alcohol bath. A solution of 7 grams of NaOH in 30 ml of water was slowly added to the mixture. A reaction occurred after 15 ml of the NaOH solution was added. A black precipitate with a small amount of bright material was formed. The material was filtered, washed, dried in air, and stored over H_2SO_4.

b) Platinum Black #73-11. Two grams of $PtCl_4$ were dissolved in 60 ml of water and 7 ml of concentrated HCl was added. To this mixture, 5 grams of NaOH dissolved in 30 ml of water were added. Finally, 20 ml of a 37% formaldehyde solution were mixed in, and the

TABLE 1.1

Sample #	Concentration of Total Mixture (moles/liter) H_2PtCl_6	HCHO	NaOH	Approximate Induction Period (min)	Temperature (°C) Initial	Final	Surface Area (m^2/g)	Comments
73-10	0.22*	2.14	1.89	---	---	---	---	Some bright material was formed
73-11	0.06*	2.42	0.95	90	---	---	---	A mirror formed
73-12	0.05‡*	2.16‡	---	---+	---	---	---	Stirring of reaction mixture caused coagulation of particles
73-13	0.07‡*	2.16‡	---	---+	11.0	17.0	10.7	A small amount of bright material was formed
73-14	0.05*	1.68	0.25	5	9.0	20.0	21.0	The solution was neutralized before an excess of NaOH was added. A small amount of bright material formed
73-15	0.03	2.34	0.57	25	9.0	22.0	26.2	A large amount of bright platelets was formed
73-16	0.05	1.50	1.00	30	10.0	23.0	24.8	Formation of bright material was extensive
73-17	0.02	1.50	1.00	15	10.0	24.0	14.6	Mirror formation was very extensive
73-18	0.02	0.15	1.00	120	10.0	23.0	12.1	Very little bright material formed
73-19	0.25	1.50	5.00	0	10.0	40.0	21.6	No bright material formed. The NaOH and $H_2(PtCl_6)$ were mixed, then the HCHO added.

* $PtCl_4$ was used instead of $H_2PtCl_6 \cdot 6\,H_2O$

‡ Refers to initial concentration of reaction mixture (before the NaOH addition)

\+ 1.0M NaOH solution was added continuously

TABLE 1.1 (Cont.)

Sample #	Concentration of Total Mixture (moles/liter) H_2PtCl_6	HCHO	NaOH	Approximate Induction Period (min)	Initial	Final	Surface Area (m^2/gm)	Comments
73-20	0.25	1.50	5.00	0	17.0	50.0	26.6	No bright material formed
73-21	0.06‡	2.05‡	---	---+	17.0	28.0	18.4	No mirror formed
73-22	0.03*	1.50	1.00	15	---	---	16.5	Reaction was followed in colorimeter
73-23	0.05	1.50	1.00	30	17.5	27.5	22.6	No stirring; the reaction spread from a mirror formed on the surface to the rest of the solution. Reaction was followed in colorimeter. (See Fig. 1.4)
73-24	0.05	1.50	1.00	0	62.5	---	11.6	A mirror formed as the reaction cooled
73-25	0.25	1.50	5.00	0	79.0	---	31.7	A small amount of bright material formed
73-26	0.25	1.50	5.00	0	100.0	100.0	3.0	N_2 bubbled during reaction. Precipitate was grey.
73-27	0.04	3.00	0.87	0	100.0	100.0	48.3	O_2 bubbled during reaction. Precipitate was greyish black.
73-28	0.23‡	2.16‡	---	---+	-10.0	-2.0	12.9	NaOH added dropwise; precipitate heated to 45°C and allowed to settle.

* $PtCl_4$ was used instead of $H_2PtCl_6 \cdot 6\,H_2O$

‡ Refers to initial concentration of reaction mixture (before the NaOH addition)

\+ 2.6M NaOH solution was added continuously

entire mixture was cooled in a dry ice-isopropyl alcohol bath. The reaction took about 1-1/2 hours to occur; on standing, a bright mirror formed on top of the reaction mixture. The material was filtered, washed, dried and stored over H_2SO_4, as were all the platinum black samples.

c) Platinum Black #73-12. One gram of $PtCl_4$ was dissolved in 50 ml of water, and 10 ml of 37% HCHO were added. The mixture was cooled to 5°C and NaOH (1N) solution was added slowly. The mixture was added slowly. The mixture was continually stirred with a magnetic stirring bar. The alkali solution was added continually to keep the pH at about 10. The temperature of the solution rose slowly to 26°C as the reaction proceeded. There was very little mirror formation. The stirring served to coagulate the particles which were easily filtered yielding a clear filtrate.

d) Platinum Black #73-13. Seven grams of $PtCl_4$ were dissolved in 250 ml of water to which 50 ml of 37% HCHO were added. The solution was cooled to 11°C. A total of 140 ml of 1N NaOH solution were added dropwise from a buret. After the addition of approximately 70 ml, the reaction appeared to start and stirring was stopped. The reaction product contained some bright material. The temperature rose to 23°C during the period under study. The substance was washed and a colloidal solution formed in the filtrate. The material was dried and stored over H_2SO_4. If there had been no reaction, the final concentration of reactants would have been as follows: (1) $PtCl_4$ = 0.05M, (2) HCHO = 1.47M; and (3) NaOH = 0.32M.

e) Platinum Black #73-14. Seven grams of $PtCl_4$ were dissolved in 225 ml of water and mixed with 50 ml of 37% HCHO solution, 35.7 ml of 1N NaOH were added to neutralize the mixture which was then cooled to 9°C. Then 75 ml of 1N NaOH were added in one dose. The reaction followed within five minutes and stirring was stopped. The initial reactant concentrations were 0.05M $PtCl_4$, 1.68M HCHO, and 0.25M NaOH. There was a moderate amount of mirror formation. The temperature rose to 20°C during the reaction.

f) Platinum Black #73-15. Seven grams of $H_2(PtCl_6) \cdot 6\ H_2O$ were dissolved in 220 ml of water to which 80 ml of 37% HCHO was added. The mixture was cooled to 9°C with an ice bath. Ten grams of NaOH dissolved in 140 ml of water and cooled to 9°C were added to the solution in one dose. The initial concentration of the reactants was 0.03M $H_2(PtCl_6)$, 2.34M HCHO, and 0.57M NaOH. Bright particles formed on the surface of the reaction in approximately 20 minutes, but the reaction in the body of the solution did not seem to start for at least 50 minutes. The product had large sheets of bright material. The temperature of the solution rose to 22°C.

g) Platinum Black #73-16. Here, 7.77 grams of $H_2(PtCl_6) \cdot 6\ H_2O$ were dissolved in approximately 50 ml of water to which 31 ml of HCHO were added. The mixture was then diluted to 160 ml and cooled to 10°C. Then, 10.56 grams of NaOH were dissolved and diluted to 100 ml which were added all at once to the 150 ml of $H_2(PtCl_6)$ and HCHO solution. The initial concentrations of reactants were 0.05M $H_2(PtCl_6)$, 1.5M HCHO, and 1.0M NaOH. The reaction proceeded slowly with the formation of a large mirror on the surface of the solution. The stirring was stopped as soon as the reaction appeared to be taking place in the body of the mixture. The temperature rose to 23°C. The material was filtered and washed. A colloidal solution of platinum black formed in the filtrate. See Fig. 1.3.

h) Platinum Black #73-17. Here 7.77 grams of $H_2(PtCl_6) \cdot 6\ H_2O$ and 89.75 ml of 37% HCHO were diluted to 400 ml and cooled to 10°C in an ice bath. Next, 30.5 grams of NaOH were dissolved in 375 ml of water and added to the reaction mixture. The initial concentrations of the reactants were 0.02M $H_2(PtCl_6)$, 1.5M HCHO, and 1.0M NaOH. The reaction appeared to have an induction period of approximately fifteen minutes. There was a great deal of bright material formed. During this time, the temperature rose to 24°C. The material was filtered and washed with a colloidal solution forming in the filtrate. Here again, the stirring was stopped once the reaction seemed to be proceeding throughout the reaction mixture.

i) Platinum Black #73-18. In this experiment, 7.77 grams of $H_2(PtCl_6) \cdot 6\ H_2O$ were dissolved in water to which 9 ml of 37% HCHO were added. The mixture was diluted to 575 ml with distilled water and cooled to 10°C with an ice bath. Two hundred milliliters of a NaOH solution containing 30.8 grams of NaOH and cooled to 10°C were added to the mixture. It took over two hours for the reaction to get started and the temperature rose to 23°C. There was very little bright material formed. The initial concentrations of the reactants were 0.02M $H_2(PtCl_6) \cdot$ 0.15M HCHO, and 1.0M NaOH. When the product was filtered and washed, a colloidal solution formed in the filtrate. Oxygen was bubbled through a glass frit into the filtrate, which coagulated the platinum black and made it filterable.

j) Platinum Black #73-19. In this reaction, 12.95 grams of $H_2(PtCl_6) \cdot 6\ H_2O$, and 20.4 grams of NaOH were dissolved in 90 ml of water. The mixture was then cooled to 10°C. Then, 11.6 ml of 37% HCHO solution were added making a total of 101.6 ml of solution (0.25M $H_2(PtCl_6)$, 1.5M HCHO, 5.0M NaOH). The reaction was immediate and extremely vigorous. The temperature rose to 40°C and the material precipitated out of the reaction mixture. The product was easily filtered and washed without any formation of a colloidal solution. There was no apparent formation of bright material.

k) Platinum Black #73-20. This experiment was practically identical to #73-19 except that the order of combining the reactants was changed. The $H_2(PtCl_6)$ and HCHO solution was mixed and then the NaOH was added. The total solution was still 101.6 ml, and the initial reactant concentrations were the same. The temperature rose from 17°C to 50°C during the reaction which again was immediate and vigorous. There was not apparent mirror formation and the material was easily filtered and washed with no colloidal solution resulting. In both reactions, no stirring was required due to the rapid reaction.

l) Platinum Black #73-21. This preparation is identical to #73-16, except that the NaOH solution was not added in one dose but dropwise from a buret (~ 2 ml/min). The reaction mixture was stirred continually throughout the addition of the base. The temperature rose from 17°C to 28°C, and a great deal of bright material formed. The material was filtered, washed, and dried in air.

m) Platinum Black #73-22. In practically every mixed electrode potential vs time plot, two distinct, small plateaus appear. In order to relate these to either nucleation or particle growth, we examined the reaction spectroscopically. One gram of $PtCl_4$ was dissolved in 50 ml of distilled water to which 11.6 ml of 37% HCHO were added, and the total solution was diluted to 80 ml. The solution was cooled to 10°C. Forty milliters of a solution containing 4 grams of NaOH were added to bring the total reaction mixture to 120 ml (0.03M $PtCl_4$, 1.5M HCHO, and 1.0M NaOH). Part of the mixture was placed in a cuvette and examined in a Klett-Summerson Photoelectric Colorimeter to obtain optical density measurements. The colorimeter used a Corning glass filter #2412 with a bandpass of 600-800 mμ. Using a Beckman DK-2 spectrophotometer, it was found that NaOH, HCOH, and $PtCl_4$ solutions do not adsorb in this region. The rest of the reaction mixture was subjected to pH and mixed electrode potential measurements. Neither solution was stirred after the initial mixing. The reaction proceeded slowly with a great deal of bright material forming on the surface of both solutions. The absorbance measurements show a continuous unbroken increase with time, while potential measurements showed the normal plateaus.

n) Platinum Black #73-23. The above measurements were repeated using chloroplatinic acid instead of $PtCl_4$. The reaction mixture was exactly the same as used in #73-16. The initial temperature of the solution was 17.5°C. A portion of the reaction mixture was placed in the colorimeter, and the pH and mixed electrode potential was measured on the rest of the solution. Neither portion was stirred after the initial mixing. The surface of the mixture became covered with a platinum mirror, while the body of the solution remained clear. Then, a darkening occurred directly

below the mirror and proceeded slowly into the body of the solution. There was a sharp demarcation between the black opaque area and the remaining clear orange-red portion of the solution, while this darkening spread to two thirds of the way down to the bottom of the reaction vessel. If the mirror were broken, it would "repair" itself so that the surface was covered completely at all times. The temperature of the main solution rose to 27.5°C during this time.

The potential versus time plot (see Fig. 1.4) shows the characteristic double plateau, yet, the absorbance curve shows no discontinuities. Both in the reduction of platinic chloride and in the reduction of chloroplatinic acid, absorbance measurements do not seem to shed any light on the reason for the potential plateaus.

The reaction product had a great deal of bright material. The substance was filtered, washed and dried.

o) Platinum Black #73-24. In this reaction, the conditions of experiment #73-16 were again repeated except that the NaOH and $H_2(PtCl_6)$ solutions were heated separately to 60°C (0.05M H_2PtCl_6, 1.5M HCHO, and 1M NaOH). First, 31 ml of 37% HCHO at room temperature were combined with the hot $H_2(PtCl_6)$ solution and then the hot NaOH solution was added. The temperature of the solution rose to 62.5°C and the reaction started immediately. As the reaction proceeded and the temperature dropped, a bright mirror formed on the surface. The final temperature was 28°C. At lower temperatures this same reaction (#73-16) took 30 minutes before anything seemed to occur, but at higher temperatures the reaction was immediate. Also, there was no colloidal solution formed on washing the precipitate.

p) Platinum Black #73-25. To find the effect of high temperatures on concentrated solutions, experiment #73-20 was repeated except that the $H_2(PtCl_6)$ and NaOH solutions were heated to 65°C. The HCHO was added to the hot $H_2(PtCl_6)$ solution and then the hot NaOH solution was added. The reaction was immediate and very vigorous. The temperature rose to 79°C and there was a small amount of bright material formed. The product was easily filtered, washed and dried.

q) Platinum Black #73-26. A mixture of 12.95 grams of $H_2(PtCl_6) \cdot 6\ H_2O$ and 20.4 grams of NaOH were dissolved in 90 ml of water which was placed in a closed reaction flask. The mixture was heated to 100°C with a water bath, while N_2 was bubbled through the solution, 11.6 ml of HCHO were added from a buret into a tube leading to the bottom of the reaction vessel. The reaction was immediate with formation of a gray precipitate. All the reactants were not consumed, as the filtrate was orange in color. The gray material was washed and dried.

r) Platinum Black #73-27. A mixture of 7.77 grams of $H_2PtCl_6 \cdot 6\ H_2O$ and 10.56 grams of NaOH were dissolved in water and diluted to 230 ml. The mixture was heated in a closed reaction vessel to 100°C with a water bath while O_2 was bubbled through the solution. Then, 31.6 ml of HCHO were added from a buret. At this higher temperature, a large portion of the HCHO was lost by vaporization; therefore, 40 ml more were added insuring an excess of reactant. The reactant concentrations were as follows: (1) 0.04 ml M H_2PtCl_6, (2) 3.00M HCHO, and (3) 0.87M NaOH. The reaction was instantaneous and the resulting product was grayish black. The material was washed, dried, and stored over H_2SO_4.

4. Discussion: The above experiments were essentially exploratory in character: the intent was to map out the general conditions leading to high surface area materials. This study will be followed by a detailed examination of selected, controlled precipitation conditions which appear promising.

The reproducibility of the material produced under given conditions has not been studied extensively. From the limited data we obtained, it appears that the surface area is fairly reproducible. For example, runs 73-16 and 73-23 made under identical conditions, gave materials of 24.8 and 22.6 m^2/g, respectively. In both cases, there was extensive mirror formation on the surface, and an induction period of 30 min.

Mirror formation appears to depend on the length of the induction period, in the sense that a long induction period favors its formation. Preparation 73-18 is an exception to this rule. In all cases where the induction

time was essentially zero, there was no mirror formation. The induction time appears to depend inversely on the H_2PtCl_6 and HCHO concentrations and directly on the NaOH concentration. Also, it depends strongly on the temperature, being essentially zero at high temperatures (60°C or above). The dependence on the platinum and formaldehyde concentrations is easily rationalized in terms of nucleation; the effect of the NaOH concentration is less clear and will be studied further.

The nature of the material precipitated as a mirror is unclear. Mirror formation does not necessarily imply that the platinum black formed under the same conditions will have a low surface area (see preparations 73-15, 73-16, 73-23). If, as reported in the literature[7], blacks precipitated under conditions where mirrors are formed are inferior catalysts, this must be due to effects other than a simple decrease of area.

In general, high surface area blacks (~ 25-30 m^2/g) can be obtained from relatively concentrated solutions of the platinum salt and formaldehyde either at low or at high temperatures. Solutions with low concentration of platinum and formaldehyde tend to yield low surface areas.

The NaOH concentration also influences the surface area: for given H_2PtCl_6 and HCHO concentrations. The surface area increases with the NaOH concentration. This dependence is illustrated by preparations 73-13, 73-14, 73-16, and 73-23. In preparation 73-13, the NaOH concentration tends to zero (dropwise addition) and the surface area was 10.8 m^2/g; at 0.25M NaOH, the area was 21.0 m^2/g; at 1.0M NaOH, the area was 23.8 m^2/g (avg. of 24.8 and 22.6 m^2/g). This dependence on NaOH concentrations is in the same sense as the dependence on H_2PtCl_6 and HCHO concentrations, i.e. the faster the reaction, the greater the surface area of the resulting black. However, it should be pointed out that the induction time at a given temperature was longer at greater NaOH concentrations (compare 73-14 and 73-16), which suggests a slower reaction rate for nucleation (as distinct from growth) at higher NaOH concentrations.

The effect of temperature seems to depend on whether we are dealing with low or high H_2PtCl_6 concentrations: at low H_2PtCl_6 (0.05M and at 1M NaOH), increasing the initial temperature from 17.5° to 62.5°C, decreased

the area from 22.6 to 11.6 m^2/g (runs 73-23 and 73-24); at high H_2PtCl_6 concentrations (0.25M and at 5.0M NaOH), the surface area increased from 21.6 to 31.7 m^2/g as the initial temperature was raised from 10.0 to 79°C (compare runs 73-19, 73-20, and 73-25). The temperature was not kept constant during the whole course of the reaction, and therefore, we can only correlate to the mean temperature during the run. This increased in the sequence of the runs 73-19, 73-20 and 73-25.

The most dramatic effect on surface area is shown by runs 73-26 and 73-27. Although there were differences in the concentrations of H_2PtCl_6, HCHO, and NaOH, the expected result was a high surface area in run 73-26 (high H_2PtCl_6 concentration) and a relatively low surface area in run 73-27 (low H_2PtCl_6 concentration). In fact, the area of the black prepared in 73-26 was only 3 m^2/g while that of run 73-27 was 48.3 m^2/g. This unexpected and large difference is essentially attributable to bubbling N_2 in the first instance and of O_2 in the second, through the solution. This result immediately suggests that the oxygen content of the solution is a critical variable in determining the surface area. There is some corroboration in the older literature, particularly from studies of the effect of adsorbed oxygen on activity. At this stage, we do not know what the origin of this effect is; speculatively, it may be suggested that O_2 functions as an inhibitor to particle growth by being chemisorbed on freshly-formed platinum surfaces. It is also possible that chemisorbed oxygen inhibits subsequent sintering or recrystallization of platinum black. The precise role of oxygen in controlling the particle size and surface area is currently under study.

The surface areas of materials prepared here varied with conditions between 3 and 48 m^2/g. These areas may be contrasted with those of commercially available material (Englehard platinum black) determined at our laboratory. Three lots of presumably identical commercial catalyst gave areas of 27, 33.3 and 40.7 m^2/g. The area of most of our preparations fall within this range but appear to be more reproducible for the same conditions of preparation. On the basis of the results of run 73-27, it appears possible to produce blacks with areas substantially greater than 40 m^2/g.

It is not known whether such materials retain their high surface area and show high catalytic activity for propane oxidation if used directly in making electrodes, i.e. unsupported. A more relevant question is whether we can produce such high surface area materials on specific supports and whether such structures will show high activity. This will be investigated in subsequent phases of the program.

IV. CHARACTERIZATION OF PLATINUM BLACKS

A. B.E.T. Measurements

B.E.T. measurements using Krypton were done on all samples, with the exception of three preliminary preparations; the results are given in Table 1.1. The B.E.T. surface area can be correlated to a particle size using the expression

$$d\,(\text{Å}) = \frac{2.8 \times 10^3}{S\,(m^2/g)}$$

assuming spherical particles. It must be kept in mind that the surface inside pores with radii smaller than a certain limit ($\sim$ 7 Å) is not seen by this method. In spite of these limitations, comparison of particle sizes calculated from B.E.T. areas with particle (or crystallite) sizes obtained by other methods (electron microscopy, shadowgraphy, selected area electron diffraction, and X-ray diffraction) gives valuable information on the homogeneity of the sample and makes it possible to tell if the elementary particles are single crystals or polycrystalline.

B. Electron Microscopy

Electron shadowgraphy gives a very good idea of the structure of the aggregates and permits an estimate of their internal porosity. However, this method does not always yield reliable values for the actual size of the particles; selected area electron diffraction and X-ray diffraction are more reliable methods in this last respect.

Shadowgraphs of blacks obtained from various preparations are shown in Figs. 1.5 - 1.8, 1.11, 1.12, 1.14 - 1.16, 1.18, and 1.19. In each case, the black was sonified in N, N-dimethylformamide or water before a shadowgraph was obtained in order to break up large, loosely adherent agglomerates; however, care was exercised to avoid introducing modifications in the basic structure of the black.

Figures 1.5 and 1.6 give a comparison between a platinum black prepared in run 73-13 with surface area of 10.8 m^2/g and commerical platinum black with an average of 30 m^2/g in surface area. It is evident that preparation 73-13 is quite extensively agglomerated and has little internal porosity compared to commercial black. This difference is reflected in the difference of surface areas.

Shadowgraphy gives an interesting insight into the nature of the particles of the aggregate when combined with selected area electron diffraction and X-ray diffraction. As was shown in the last interim report, a combination of shadowgraphic particle counting with crystallite size determination (diffraction methods), made it possible to demonstrate that the particles in the aggregate of Fig. 1.6 are basically single crystals. In the case of preparations consisting of "black" and "bright" (mirror) materials, as in preparation 73-15, it is possible to obtain information on the nature of the different materials. Figure 1.7 shows that the black material consists of particles of the same order of magnitude as those of Fig. 1.6 (note difference in scale). Figure 1.8 shows that bright material obtained from the same preparation is strongly agglomerated. The difference is clearer when using selected area electron diffraction. While the black material is made of extremely small particles showing no spots in the diffraction pattern (Fig. 1.9a), the bright material shows distinct spots in the pattern (Fig. 1.9b). By counting the distribution of spot sizes in a given ring, an average crystallite size of 42 Å can be calculated for this material (Fig. 1.10). This value was confirmed by X-ray diffraction, which gave an average crystallite size of $d = 45 \pm 3$ Å. The nature of this preparation with very different components may explain why the equivalent B.E.T. diameter, d = 108 Å, differs from the above value calculated from electron and X-ray diffraction patterns. This could also indicate that the particles are not single crystals.

Figure 1.11 shows another example of a preparation with a relatively open structure halfway between that of Figs. 1.5 and 1.6.

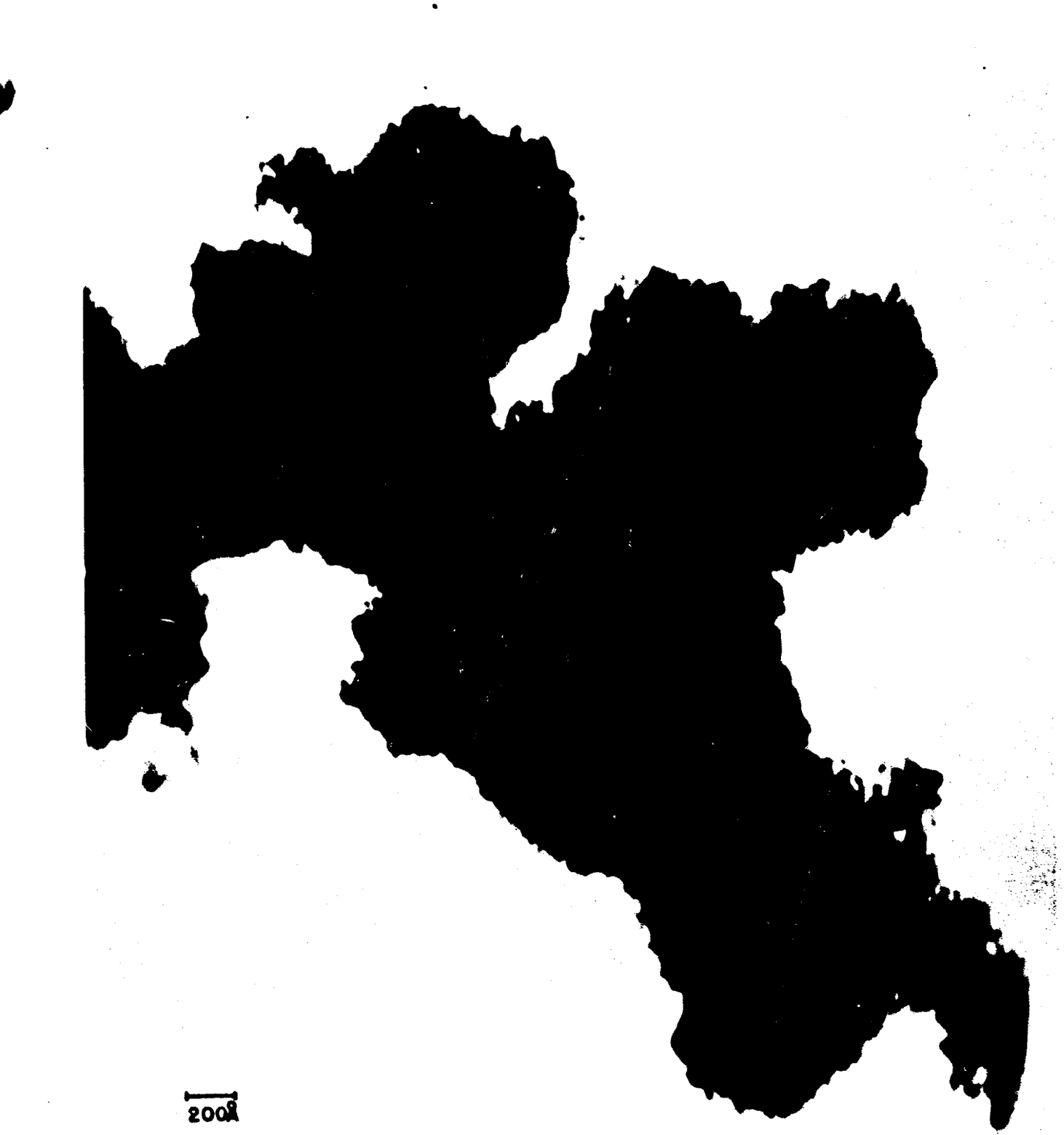

Fig. 1.5 Pt black #73-13 (500.000X) after sonification in N, N-Dimethylformamide for 5 minutes.

Fig. 1.6 Commercial Pt black (500.000X).

Fig. 1.7 Pt black #73-15 (200,000X) after sonification in N, N-Dimethylformamide for 5 minutes.

Fig. 1.8 Pt black #73-15 (200,000X) after sonification in N, N-Dimethylformamide for 20 minutes.

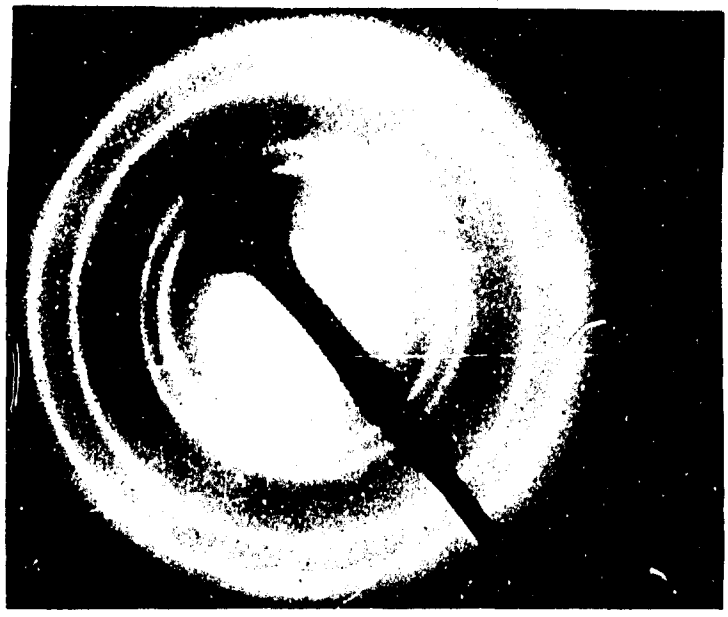

(a)

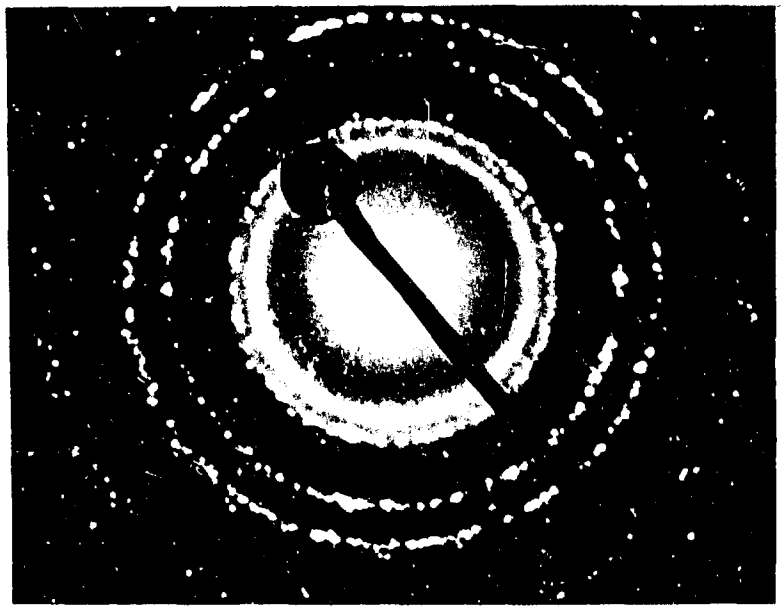

(b)

Fig. 1.9 Selected area diffraction patterns of Pt black #73-15.

Fig. 1.10

Cumulative log-probability distribution of particle size of Pt black #73-15 (from electron diffraction patterns).

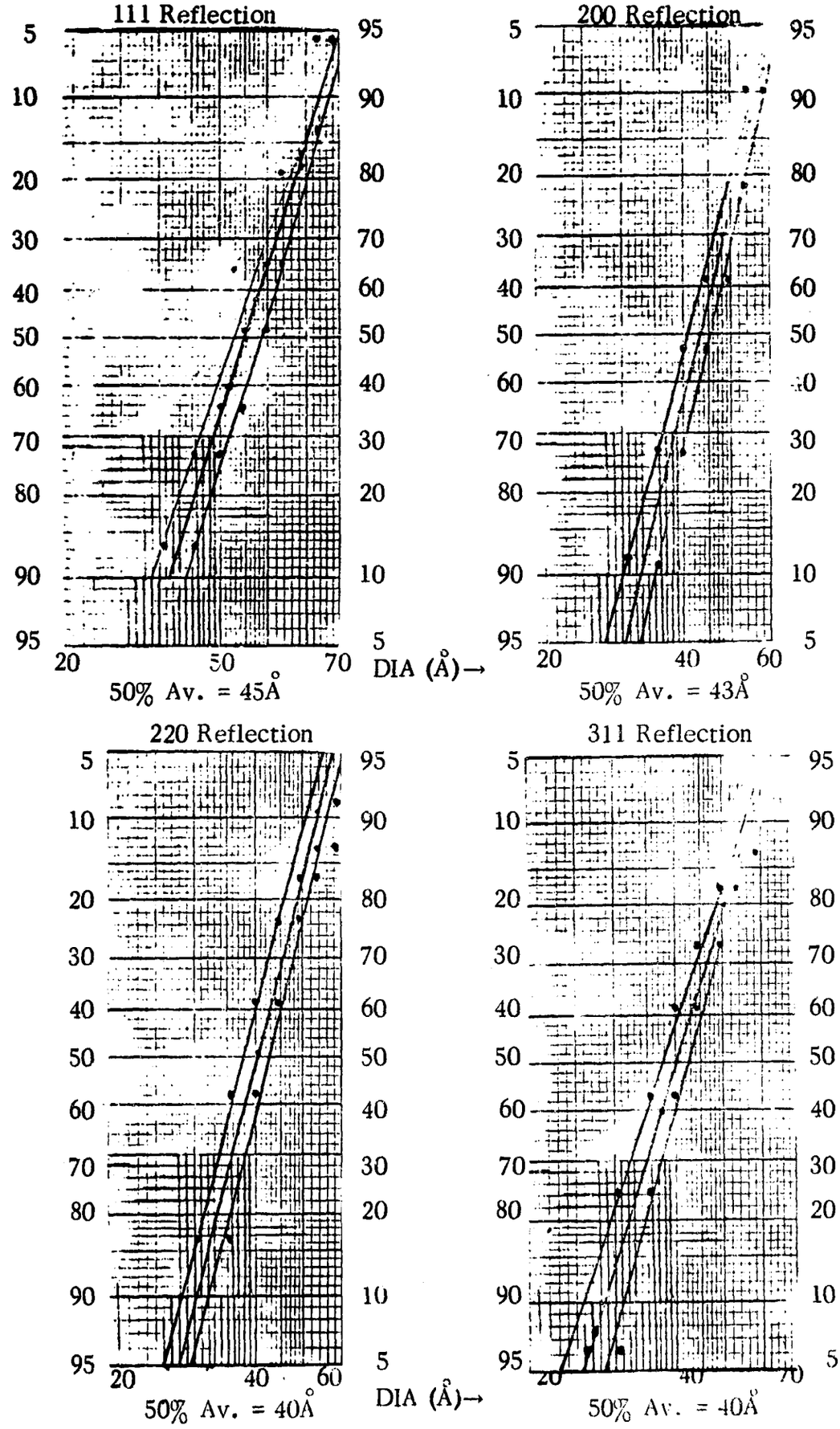

Fig. 1.11 Pt black #73-16 (500,000X) after sonification in N, N-Dimethylformamide for 20 minutes.

Figure 1.12 shows a very fine material with some large particles of irregular contours. Electron diffraction patterns (Fig. 1.13) indicate very small crystallites (continuous ring) plus a very few, large crystals. Comparison of B.E.T. particle size (d = 130 Å) with the electron diffraction pattern indicate that, also, in this case the particles as seen by B.E.T. are polycrystalline.

The series of shadowgraphs shown in Figs. 1.14 to 1.16 represent successive enlargements of a representative sample of preparation 73-26, which had a B.E.T. area of only 3 m^2/g. All through the picture, spheres of different sizes, alone or agglomerated, are observed. More accurate observation of the sphere contours shows sharp corners indicating some faceting. At the highest resolution (Fig. 1.16), clear geometric forms are observed (see arrow); a hexagon may indicate the 111 plane of a cubic crystal or a double twin. In addition, some roughness is observed in the surface which in part may be faceting. Selected area diffraction (Fig. 1.17) on a single particle of 700 Å diameter shows that these spheres are polycrystalline. The fact that some of the spots of this electron diffraction pattern are elongated may be an indication of elongation in the particular plane.

From Figs. 1.14 to 1.17 discussed above, it can be concluded that, in this case, the nuclei grow first to a single crystal and immediately afterwards compact deposition with strong intergrowth occurs in preference to dendritic growth of new crystals; the result is similar to the case of a compact electrodeposit. The particles grow as spheres because there is no preferred direction and material diffusion is spherical.

Figure 1.18, obtained from a sonified dispersion of preparation 73-27, shows a spongy material of considerable smaller particle size than the commercial material of Fig. 1.6. This material, prior to sonification, forms large spongy aggregates (Fig. 1.19). X-ray diffraction shows average crystal sizes of 70 $\pm$ 10 Å (reflection 111), 55 $\pm$ 10 Å (reflection 200), 57 $\pm$ 10 Å (reflection 220) and 58 $\pm$ 10 Å (reflection 311). These values, with the exception of the 111-reflection which is usually too high, are in good agreement with B.E.T. estimated particle size of 58 Å.

Fig. 1.12 Pt black #73-19 (200,000X) after sonification in N, N-Dimethylformamide for 20 minutes.

Fig. 1.13 Selected area diffraction pattern of Pt black #73-19.

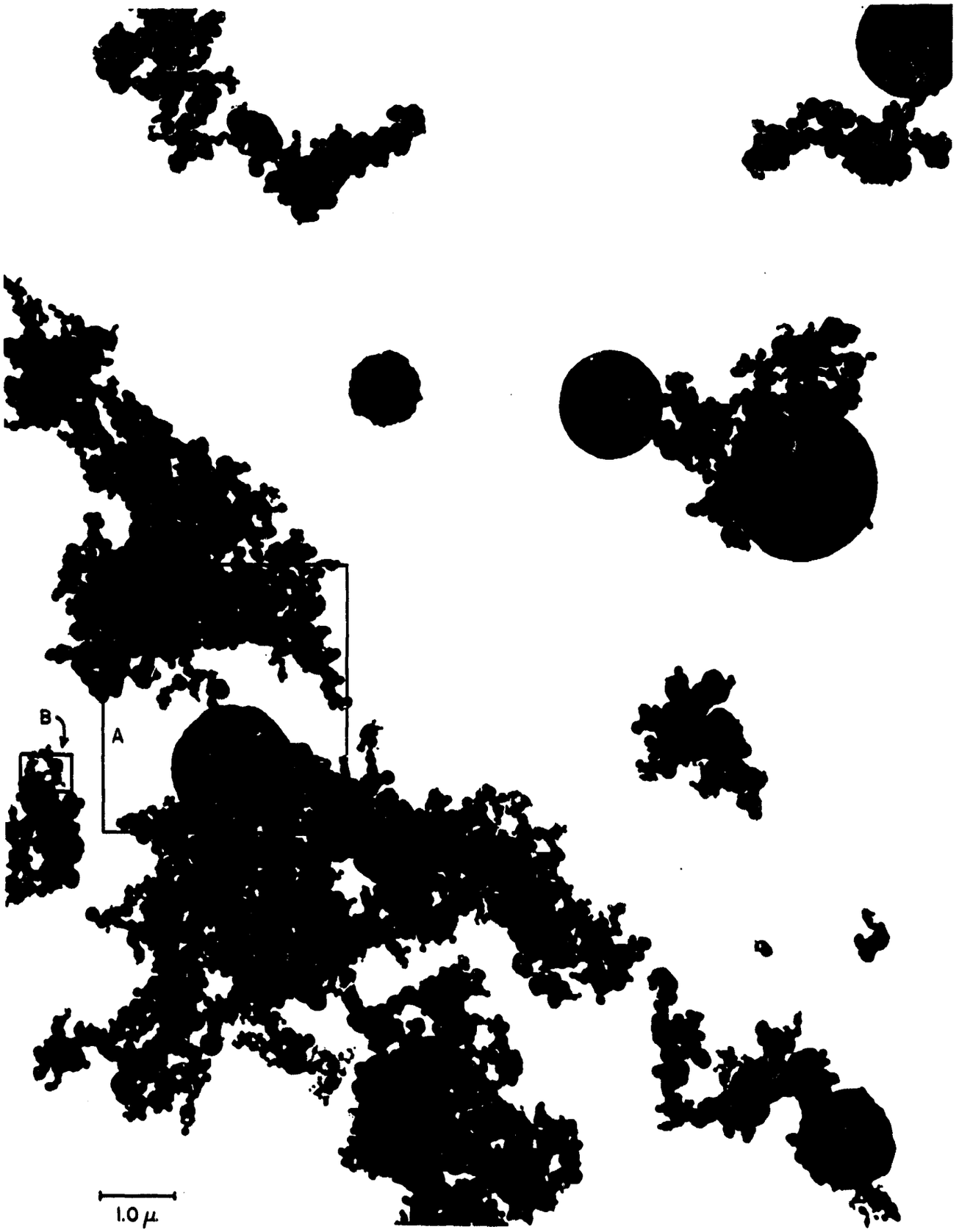

Fig. 1.14 Pt black #73-26 (15.000X) as a dry powder.

Fig. 1.15 Pt black #73-26 (75.000X) as a dry powder [area A of Fig. 1.14].

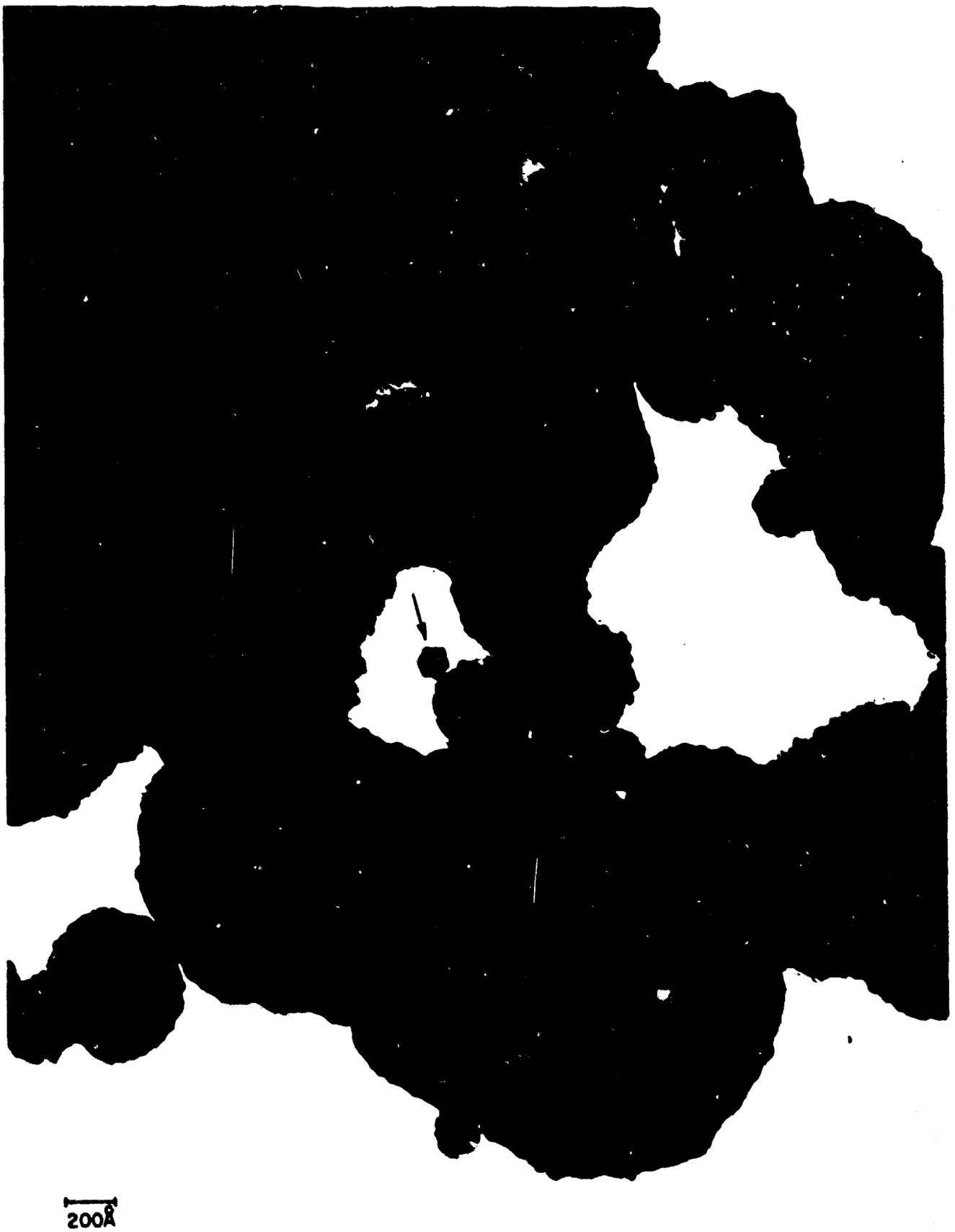

Fig. 1.16 Pt black #73-26 (500.000X) as a dry powder [area B of Fig. 1.14]

Fig. 1.17 Selected area diffraction pattern of Pt black #73-26.

Fig. 1.18 Pt black #73-27 (500.000X) after sonification in water for 30 minutes.

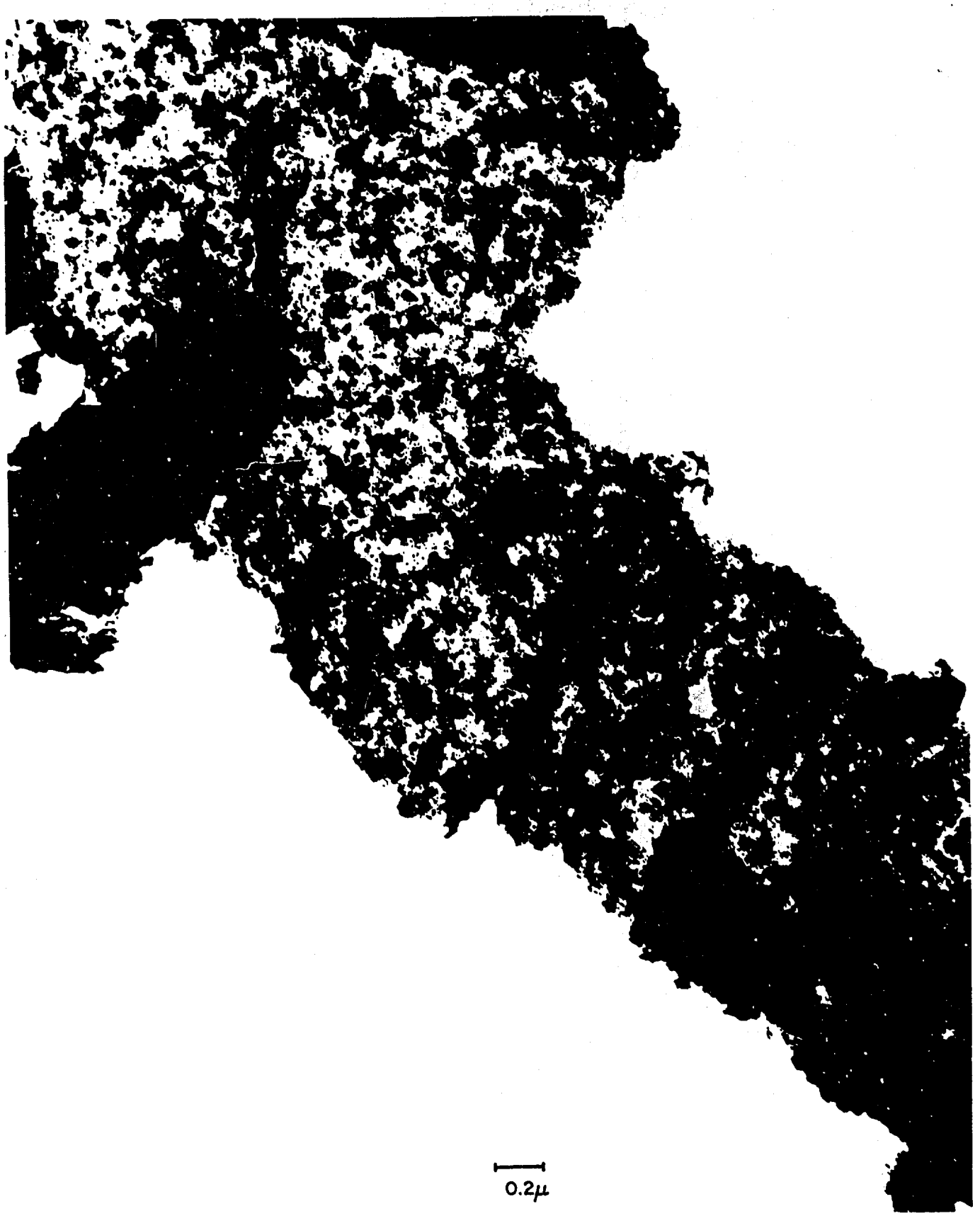

Fig. 1.19 Pt black #73-27 (50,000X) as a dry powder.

This material seems to be a mixture of a black and a gray fraction; separation and characterization of these fractions is underway.

The results discussed above are summarized in Table 1.2. Characterization of other materials prepared in the course of this program is underway and will be reported later.

C. X-ray Diffraction Studies

1. Average value of physical properties: During the period of this report the method of Warren and Averbach[44, 45] has been applied to the determination of the average values of physical properties of platinum blacks. This technique utilizes a Fourier analysis of X-ray intensity data to provide information on the average particle size, strain and strain energy, faulting, and twinning. The method has been developed in such a way that intensity data for any sample of the black may be fed directly into a computer program to yield the desired values.

X-ray powder pattern peaks for several specimens of platinum black were measured with a Norelco diffractometer equipped with a pulse-height analyzer and gas flow proportional counter, using copper Kα radiation (1.5418 Å). The diffractometer was connected to a step-scanning device by which the X-ray intensity at intervals of 0.02° (2 θ) was recorded in terms of the time taken to complete 2000 counts. These data were recorded on paper tape by a method designed and developed in this laboratory for direct conversion to IBM computer input. This method eliminates the tedious intermediate step of manual conversion of recorder output to IBM punched card data.

The intensity profile of X-ray diffraction lines of a platinum black specimen is broadened and changed by instrumental characteristics as well as by the structure-associated parameters. The Stokes method[46] of analysis of a diffraction peak separates this instrumental broadening from the rest of the pattern so that such parameters as strain, twinning, faulting, particle size, and size distribution[47, 48] can be derived.

The observed X-ray intensity h (x) at a distance x from an arbitrary reference point is related to the intensity f (x) that would appear at that point in the absence of instrumental broadening by

TABLE 1.2

Particle and Crystallite Sizes of Platinum Blacks

Preparation	BET Area (m^2/g)	BET Particle Size (Å)	Crystallite Size From X-Ray Line Broadening (Å)	Crystallite Size from Electron Diffraction Spot Counting (Å)	Remarks
Commercial	30 (avg)	100	105	100	Particles are single crystals.
73-13	10.8	---	---	---	Mixture of bright and black material. Polycrystalline and single crystal material
73-15	26.2	108	45	42	Polycrystalline particles
73-19	21.6	130	---	---	Polycrystalline particles
73-26	3.0	930	---	(<< 700)	Particles are polycrystalline
73-27	48.3	58	60 ± 10	---	Particles are single crystals
73-28	12.9	290	80 ± 10	---	Polycrystalline particles

$$h(x) = \int_{-\infty}^{\infty} f(y)\, g(x-y)\, dy$$

where g (x) is the intensity produced by crystallites large enough to exhibit no small-size effects and all the broadening is instrumental. The function f, which we wish to determine, is called the convolution of g with h. If g and h are expressed as Fourier series

$$h(x) = \sum_{t} H(t)\, e^{-2\pi ixt/a}$$

$$g(x) = \sum_{t} G(t)\, e^{-2\pi ixt/a}$$

then it can be shown that the corrected peak f (x) is represented by

$$f(x) = \sum_{t=-\infty}^{t=+\infty} F(t)\, e^{-2\pi ixt/a}$$

where

$$F(t) = \frac{H(t)}{aG(t)}$$

Since h (x) (the diffracted intensity of the sample under discussion) and g (x) (the diffracted intensity of a standard annealed sample) are known numerically, their Fourier series can be computed and the required Fourier coefficients describing broadening due to particle size and strain can thus be obtained.

The diffracted intensity at an angle θ produced by a given reflection in the absence of instrumental broadening is then represented as

$$p'(2\theta) = \sum_L A_L \exp(2\pi i L(s-s_c))$$

where s and s_o are, respectively, the position under consideration and the peak position, both in reciprocal space; $s = 2\sin\theta/\lambda$: $s_o = 2\sin\theta_{max}/\lambda$. The Fourier coefficients A_L are expressible as products of A_L^{PF}, the particle size faulting coefficient, and A_L^D, the distortion coefficient due to strain.

The strain coefficients A_L^D can be expressed by the relation

$$A_L^D = \exp(-2\pi^2 L^2 < \epsilon_L^2 > /d^2)$$

Here, $< \epsilon_L^2 >$ is the mean-square strain at a perpendicular distance L from the (hkl) plane under consideration, and d is the interplanar spacing:

$$d^2 = \frac{a^2}{h^2 + k^2 + l^2} \equiv \frac{a^2}{h_o^2} \quad \text{(for cubic crystals)}$$

It thus follows the relation

$$\ln A_L = \ln A_L^{PF} - 2\pi^2 L^2 < \epsilon_L^2 > \frac{h_o^2}{a^2} \qquad (1)$$

The Fourier coefficients obtained by computation are actually A_n where for the given range of angles $n = L/a'$ and a' are expressed by

$$a' = \lambda/2\,(\sin\theta_{max} - \sin\theta_{min})$$

The A_n values are then plotted as a function of L for each reflection so that the desired values of A_L may be obtained. This is illustrated in Figs. 1.20 and 1.21 which show the Fourier coefficients for, respectively, platinum black obtained from Engelhard Industries and platinum black prepared by formaldehyde reduction in this laboratory.

When $\ln A_L$ is plotted as a function of h_o^2 for each value of L, it is clear from Eq. (1) that the intercept value of $\ln A_L$ at $h^2 = 0$ gives the L-th particle size faulting coefficient, A_L^{PF}. Figs. 1.22 and 1.23 illustrate, respectively, such plots for the Engelhard black and the formaldehyde-reduced specimen.

Once the particle size faulting coefficients are known, Eq. (1) can be solved for the mean-square strain in each (hkl) direction:

$$\langle \epsilon_L^2 \rangle_{hkl} = \ln \frac{A_L^{PF}}{A_L} \quad \frac{a^2}{2\pi^2 L^2 h_o^2} \tag{2}$$

which gives the most accurate results for small values of L.

When the particle size faulting coefficients are plotted as a function of L, the intercept of a line parallel to the initial slope (and equal to one at $L = 0$) is termed the average effective particle size $\langle D_2 \rangle$ [1]. Figures 1.24 and 1.25 illustrate this technique for the two samples of platinum black. This average diameter includes the effects of stacking and twinning faults, which may be evaluated so that the true average particle size may be obtained.

As well as contributing to peak width, stacking and twinning faults result in shifts in the position and asymmetry of the diffraction peaks, which vary for different reflections. The annealed specimen used as a standard in these measurements shows virtually no such faulting, (as

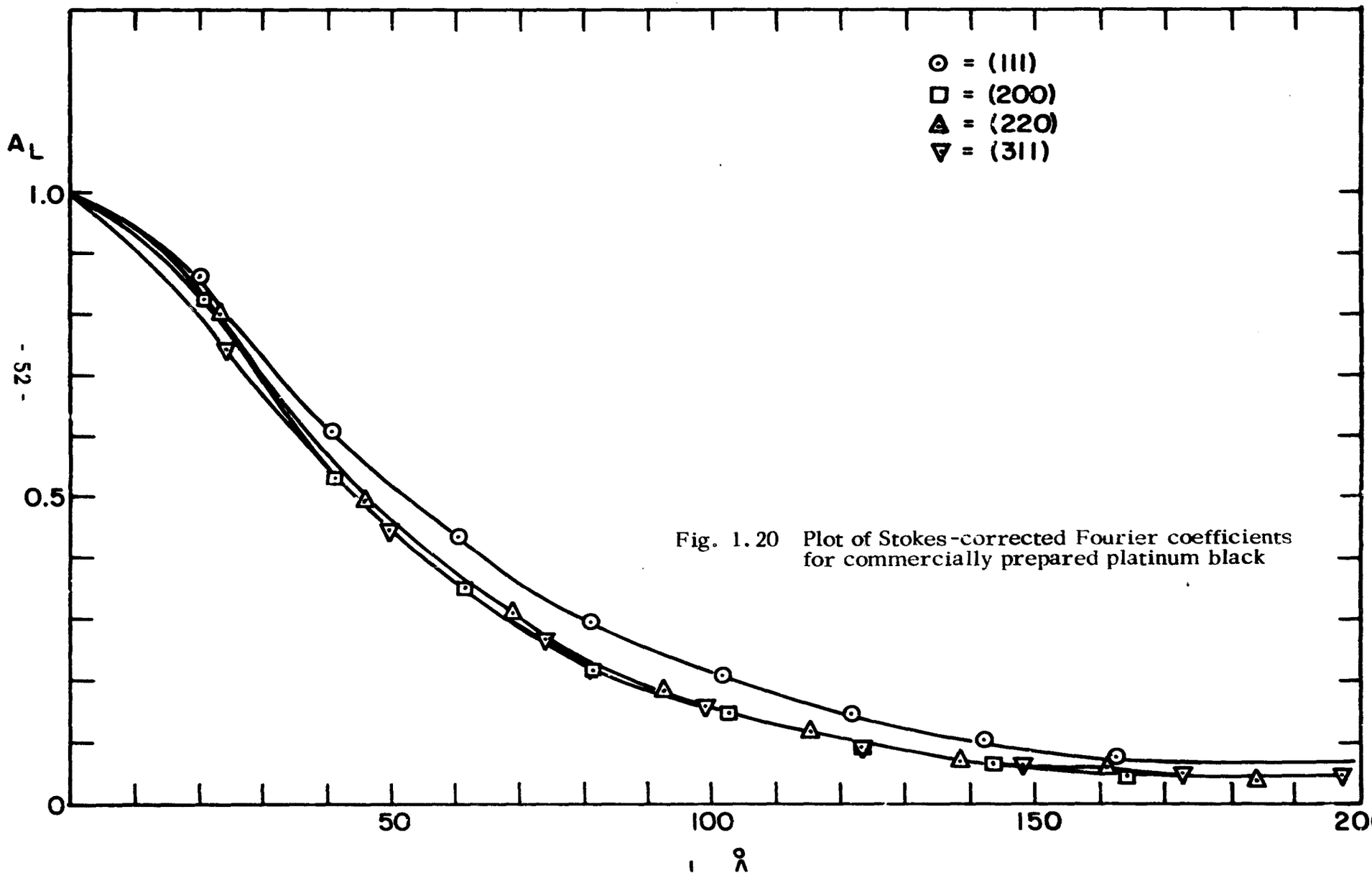

Fig. 1.20 Plot of Stokes-corrected Fourier coefficients for commercially prepared platinum black

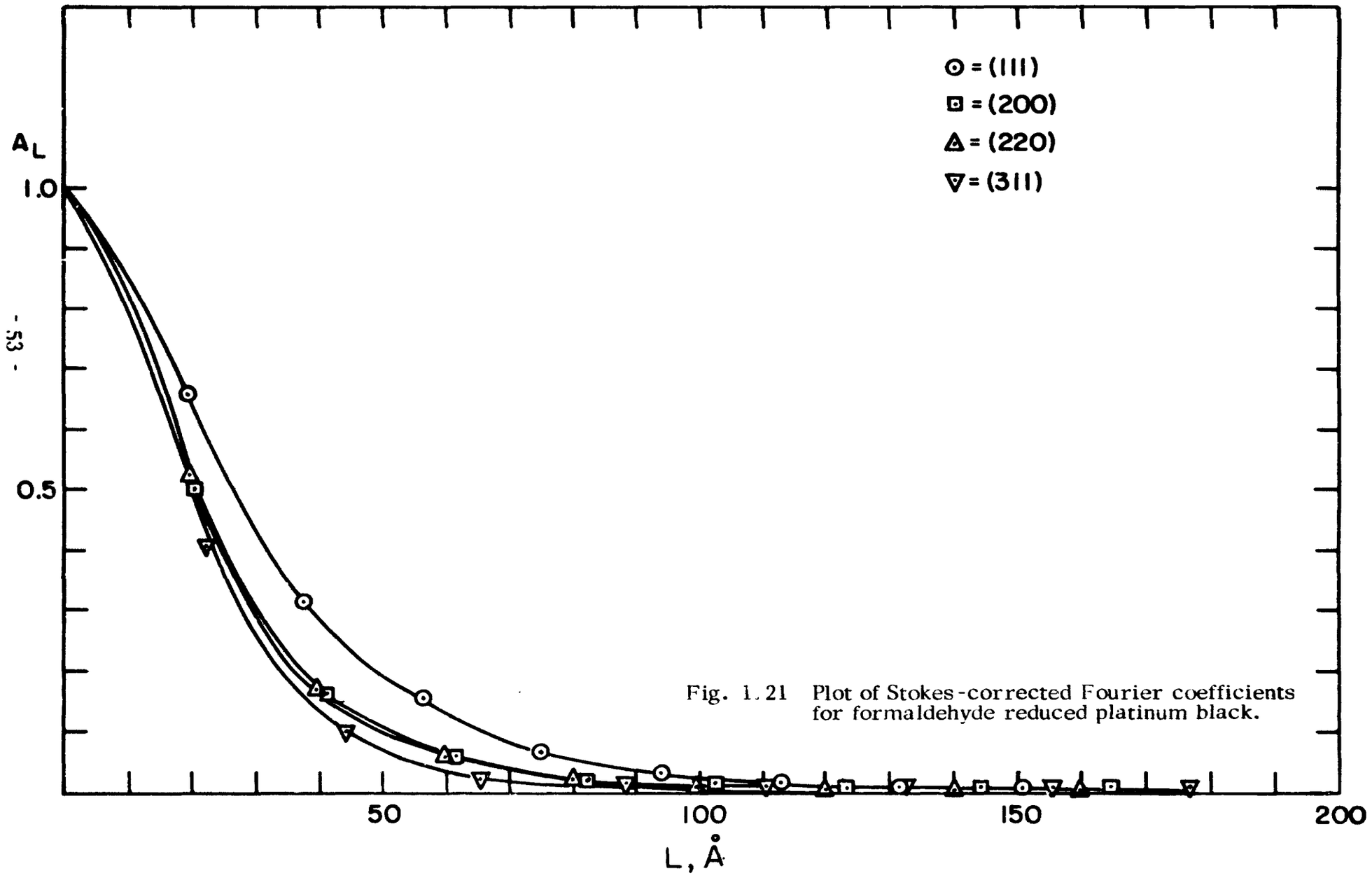

Fig. 1.21 Plot of Stokes-corrected Fourier coefficients for formaldehyde reduced platinum black.

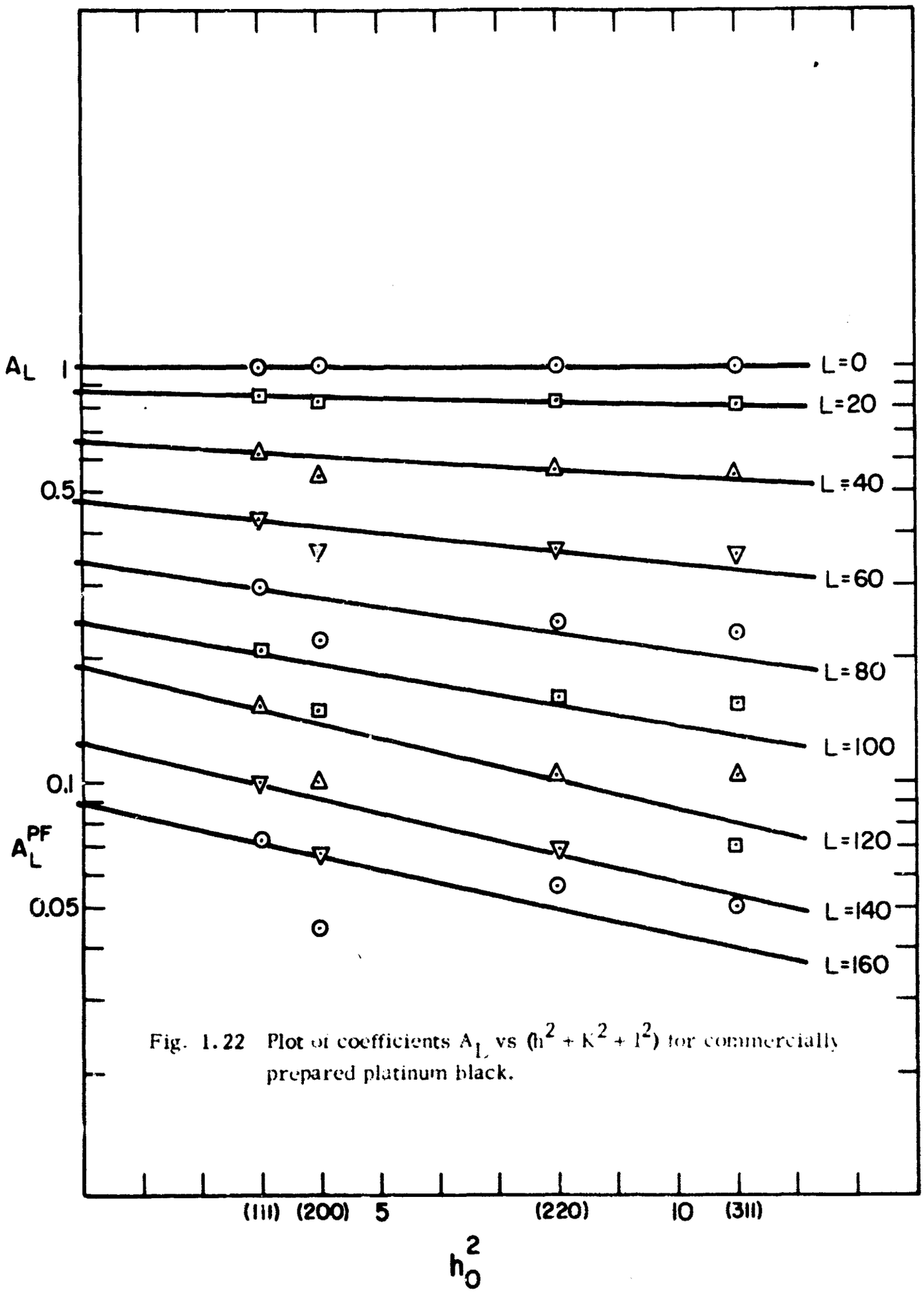

Fig. 1.22 Plot of coefficients A_L vs $(h^2 + K^2 + l^2)$ for commercially prepared platinum black.

Fig. 1.23 Plot of coefficients A_L vs $(h^2 + K^2 + l^2)$ for formaldehyde reduced platinum black.

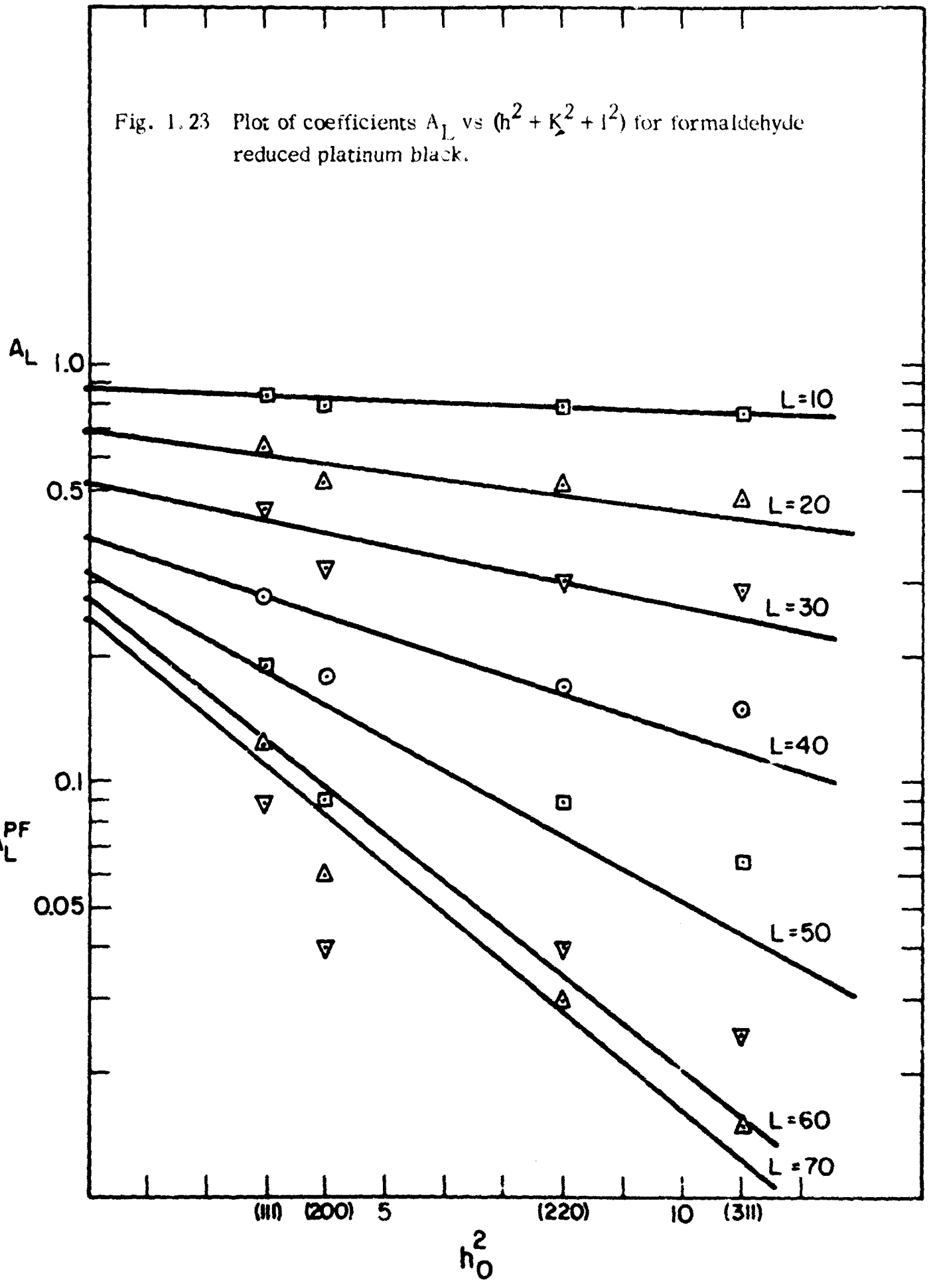

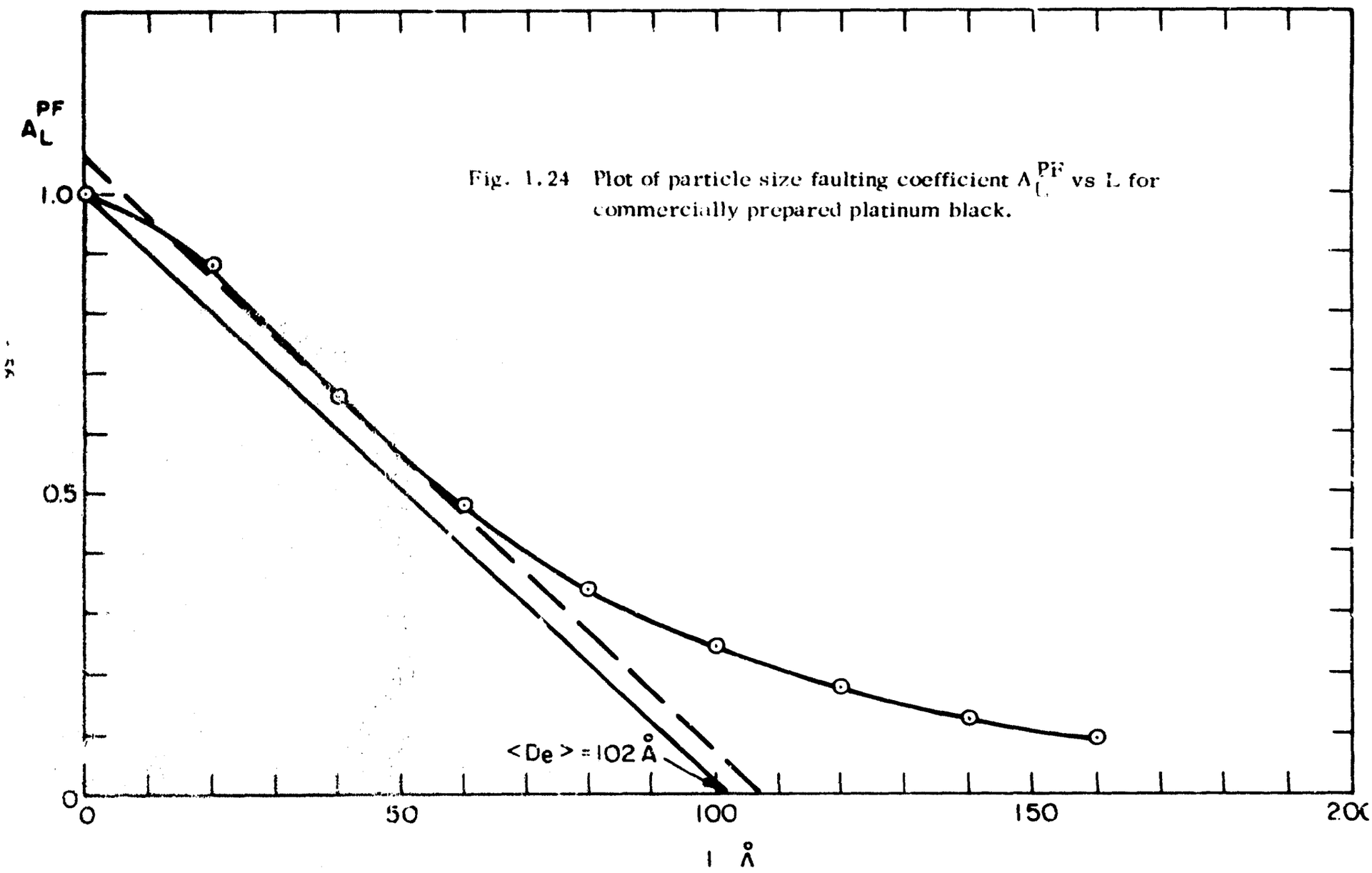

Fig. 1.24 Plot of particle size faulting coefficient A_L^{PF} vs L for commercially prepared platinum black.

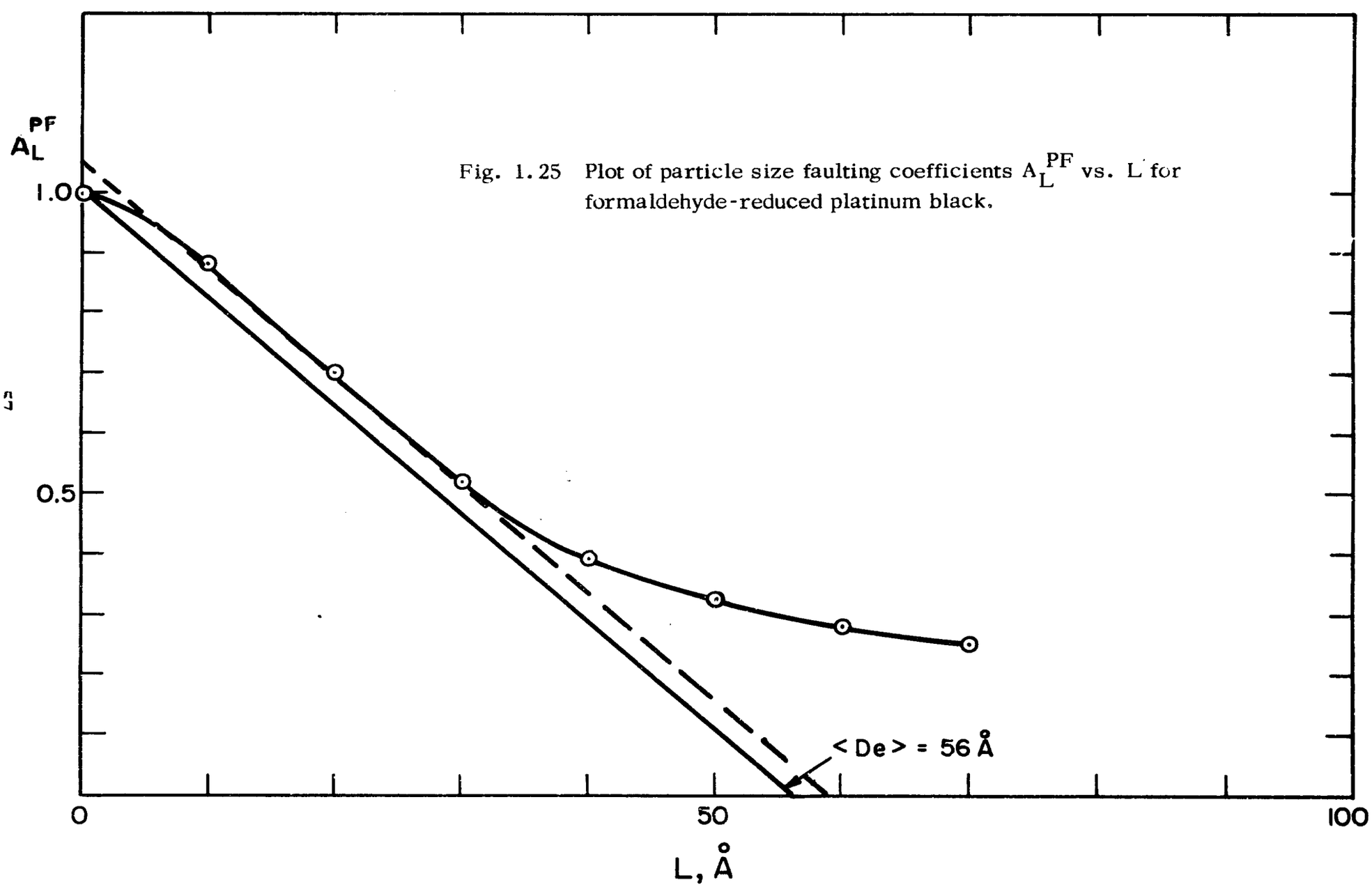

Fig. 1.25 Plot of particle size faulting coefficients A_L^{PF} vs. L for formaldehyde-reduced platinum black.

indicated by lattice constant measurements) and so the relative peak positions for two reflections may be compared for the sample and the standard to determine the stacking fault probability in the sample. The twin fault probability was evaluated from the displacement of center of gravity from the peak position.

Considering the (111) and (200) reflections for the sample and the annealed standard, the following relations are valid for face-centered cubic material[44, 49]

$$\Delta (2\theta^\circ_{200} - 2\theta^\circ_{111}) = -\frac{45\sqrt{3}\,\alpha}{\pi^2}(\tan\theta_{200} + \tfrac{1}{2}\tan\theta_{111}) \qquad (3)$$

$$\Delta CG(^\circ 2\theta_{111}) - \Delta CG(^\circ 2\theta_{200}) = \beta\,(11\tan\theta_{111} + 14.6\tan\theta_{200}) \qquad (4)$$

Here, α and β are, respectively, the probabilities of finding a stacking fault and a twin between two (111) layers. $\Delta(2\theta^\circ)$ is the difference in peak position between the sample and the standard, $\Delta CG(^\circ 2\theta)$ is the difference between the peak position and the center of gravity of the sample, and θ_{hkl} is the Bragg angle for the hkl reflection of the sample. Since these values are all measurable from the diffraction patterns, the parameters α and β can be evaluated.

Once these values are known, the actual particle diameter in each direction may be found from the relations[49] valid for isotropic material:

$$\frac{1}{\langle D_2\rangle} = \frac{1}{\langle D\rangle_{111}} + \frac{1.5\alpha+\beta}{a}\cdot\frac{3}{4}$$

$$\frac{1}{\langle D_e\rangle} = \frac{1}{\langle D\rangle_{200}} + \frac{1.5\alpha+\beta}{a}$$

$$\frac{1}{\langle D_e \rangle} = \frac{1}{\langle D \rangle_{200}} + \frac{1.5\,\alpha + \beta}{a} \cdot \frac{1}{2}$$

$$\frac{1}{\langle D_e \rangle} = \frac{1}{\langle D \rangle_{311}} + \frac{1.5\,\alpha + \beta}{a} \cdot \frac{3}{11}$$

From the mean-square strain in each (hkl) direction found by the Warren-Averbach method, the stored energy due to lattice strain may be found by[50]

$$V_{hkl} = \frac{15\,E_{hkl}}{2\,(2 - 4\nu + 8\nu^2)} \langle \epsilon^2 \rangle_{hkl}$$

where E is Young's modulus in the direction of deformation and ν is Poisson's ratio.

2. Results and Discussion. Commercial platinum black and two platinum blacks prepared by us have been studied by the X-ray techniques described above with the results given in Table 1.3.

The results given in Table 1.3 include the average, effective crystallite size which depends on the actual crystallite size $\langle D \rangle$, and the energy in each crystal:

$$\frac{1}{\langle D_e \rangle} = \frac{1}{\langle D \rangle} + \frac{1}{\langle D_F \rangle}$$

Values of $\langle D \rangle$ for the commercial material average 115 Å; for platinum blacks obtained here the corresponding values are 45 Å and 80 Å.

The stored energy ranges from an average of 0.09 cal/g for the commercial material to 0.20 cal/g. Expressed in cal/mol these values yield 3 to 40 cal/mol. To put these values in context, we may note that the stored energy of a metal crystal, such as nickel, deformed by three

TABLE 1.3

X-Ray Line Broadening Studies of Platinum Blacks

Reflection	Average Effective Crystallite Size (A) $\langle D_e \rangle$	Average Crystallite Size (A) $\langle D \rangle_{hkl}$	RMS Strain $\langle \epsilon^2 \rangle^{\frac{1}{2}}$	Stored Energy (Cal/g)	Stacking Fault Probability α	Twin Probability β
A. Commercial Platinum Black						
111		111.0	3.136×10^{-3}	0.088		
200	102	125.6	4.450×10^{-3}	0.178	0.00207	0.00411
220		117.6	3.001×10^{-3}	0.081		
311		111.5	2.847×10^{-3}	0.073		
B. Preparation 73-15						
111		42	1.087×10^{-3}	0.0106		
200	38	48.7	1.064×10^{-3}	0.0102	0.00933	0.00872
220		45	1.305×10^{-3}	0.0153		
311		42.2	1.626×10^{-3}	0.0238		
C. Preparation 73-28						
111		68.7	4.562×10^{-3}	0.187		
200	56	97.7	5.913×10^{-3}	0.315	0.0135	0.0097
220		80.2	5.562×10^{-3}	0.278		
311		69.4	4.356×10^{-3}	0.171		

successive compressions of 25% each perpendicular to the previous one is only 0.5 cal/g or 30 cal/mol. Therefore, it is apparent that the stored energy of these materials is very high and it varies substantially with preparation. It is probable that the stored energy is an important parameter in determining both catalytic activity and stability (in terms of sintering). However, a correlation, if any, between the stored energy and the catalyst properties must be deferred until our data are more extensive. (See Appendix for the Stokes analysis of diffraction peaks for IBM 7094.)

V. ACTIVITY TESTS

As discussed in the previous interim report, the most convenient method to date of testing the activity of the Pt-black for propane oxidation is to manufacture a practical pasted screen electrode (made from Pt-black and Teflon powder and pasted and sintered on a Ta-screen)[52, 53] and test it as C_3H_8 anode in 85% H_3PO_4 at 150°C[54]. A "floating electrode" arrangement[55] is used in the test cell.

A. Electrode Preparation

Pasted screen microelectrodes of approximately 1 cm^2 surface are required for the "floating electrode" measurements.

Initial preparations were attempted on a 25 mesh expanded tantalum screen. After trying many different techniques for spreading the Pt-Teflon mixture on the screen (spraying, brushing, spreading with a spatula, etc.), it was found that the expanded screen would not retain the platinum black. The mesh was too small and the expanded screen contours would not hold the black without the use of a large amount of Teflon. After changing to a 50 mesh, webbed tantalum screen of 3 mils wire, this difficulty was overcome. In order to eliminate problems arising from the poor electrical conductivity of tantalum oxide, the Ta-screen is Au-plated prior to the preparation of the electrode. The screen is first etched in a solution containing HF (6.5 wt %), HNO_3 (14 wt %), H_2SO_4 (64 wt %) and water (15.5 wt %)[56]. Afterwards, a piece of screen of about 6 cm x 6 cm is plated in a $AuCl_4$ solution (3 g/ 100 ml) 2 ma/cm^2 for five minutes using two gold foils as anodes.

Since it is difficult to prepare microelectrodes with an exactly preset amount of Pt, it is necessary to determine the weight per surface unit of the Ta screen and the accurate ratio of Pt to Teflon. From this value, the exact amount of Pt can be determined from the weight of an electrode of known dimensions.

In order to determine the weight of Ta screen per cm^2 the piece of Ta screen is washed and dried after plating and then weighed.

To determine the accuracy of this calculation, several round pieces of screen 1.2 cm in diameter were punched out and weighed. The weights agreed closely with the estimated value (from the total weight of the initial piece of Ta-screen) and gave an average of 33.1 $\pm$ 0.4 mg ($\pm$ 1.3%).

Once the screen has been cleaned and weighed, a mixture of Pt-black and Teflon is applied. A total amount of Pt is weighed to approximate a preset amount per cm^2 in the finished electrode. Preparation of electrodes with an exact preset amount of Pt per cm^2 is difficult because of losses during mixing, zones of inhomogeneous distribution in the piece from which the microelectrode is cut, etc. Therefore, the actual amount is determined after making the electrode.

The Teflon powder is mixed by adding to the Pt an estimated volume of Teflon suspension of known concentration. The percentage of Teflon in the mixture can be changed intentionally from case to case, but for standard preparations a mixture containing 30 wt % of Teflon has been selected. In order to determine accurately the ratio Teflon/Pt, which is necessary in calculating the weight of Pt, an accurate determination of the amount of Teflon added with the suspension is needed. In initial experiments, the amount of Teflon suspension to make the Teflon approximately 30 wt % of the total was controlled by adding a given number of drops from a dropper. Afterwards, we found that the deviation of weight with this method was too large. Addition with a 1 ml pipette graduated in 0.01 ml divisions gives a much more accurate addition of Teflon and this method will be used in the future. The average deviation is only $\pm$ 1.6%.

To test whether the suspension contains the amount (59.7 wt %) of Teflon claimed by the manufacturer, ten gram samples were dried and the weight of solid material determined. Values of 52.5 and 56.0 wt % were found from two different samples instead of 59.7 wt % as claimed. Therefore, small amounts to be consumed in one to two weeks will drawn from a one gallon container of bulk dispersion, analyzed, put in a closed glass container and homogenized prior to use.

The mixture made of Pt black and Teflon suspension is rolled flat between two pieces of Teflon sheet to produce an area equivalent to that of

the Ta screen (usually 10 cm^2). The tantalum screen is then placed over the paste and the paste forced into the webbed structure of the screen. Using this approach, it is possible to distribute homogeneously the desired approximate amount of platinum per electrode.

A metal punch is used to obtain circular electrodes once the paste is attached firmly to the screen. The area of each electrode is measured separately, since repeated use and resharpening of the punch tends to change its size slightly. The electrodes are dried in a vacuum oven for one hour at 50°C under air and then at 100°C for one hour under vacuum. This procedure is designed to remove slowly the water and wetting agent in the Teflon dispersion.

After drying, the electrodes are sintered in a furnace at 250-275°C for five minutes under an inert argon atmosphere. The furnace is based on a translucent quartz tube of 9.7 cm I.D. with a cold and a hot zone. It takes the furnace approximately 20 minutes to reach 250°C from room temperature, sinter, and cool down. The electrodes are placed in an aluminum cup, put into the furnace, and the argon flow and the heaters are started. When the required temperature is reached (as determined by a thermocouple) the electrodes are sintered for 5 minutes, the heaters are then turned off and the oven cooled down. When the electrodes are taken out, they are tested for water repellency. Then they are weighed and the amount of platinum and Teflon on each electrode is calculated.

The average deviation in the calculation of the actual amount of Pt in an electrode containing about 20 mg of Pt/cm^2 and 30% Teflon is the sum of 0.4 mg (error in the calculation of the weight of Ta-screen) plus 0.13 mg (error in the calculation of Teflon weight), i.e. an over-all deviation of about 0.53 mg or 3%.

Table 1.4 shows the analysis of several electrodes made on Engelhard Pt-black. The amount of Pt has been varied between 9 and 23 mg in order to compare with electrodes made from our Pt blacks. The percent Teflon is nearly constant, at approximately 30%. The results obtained with some of these electrodes are described below.

TABLE 1.4

Composition of Platinum Black Electrodes

Electrode	Weight of Platinum (mg)	Weight of Teflon (mg)	Weight % Teflon
1	19.4	8.7	30.8
2	21.6	7.2	25.0
3	22.3	9.6	30.0
4A	15.6	6.2	28.6
4B	15.6	6.3	28.6
4C	15.4	6.1	28.6
5A	15.1	6.4	30.0
5B	16.5	7.0	30.0
5C	14.2	6.1	30.0
5D	19.6	8.4	30.0

B. Electrochemical Measurements

1. Apparatus and Experimental Procedure. The "floating electrode cell" assembly mentioned in the last interim report was built, tested and used during this period. A diagram of the assembly is shown in Fig. 1.26. The cell container is a 2 liter resin reaction kettle with a cover having four 24/40 ground joints, through which the electrode holder - reference electrode assembly, the gas inlet, the gas outlet and the counter electrode are fitted.

The pasted screen (working) electrode, in the form of a circular disc approximately 1 cm^2 in area, is supported in the electrode holder on a ring of Pt wire of 0.9 in diameter and kept in position by the slight

FLOATING ELECTRODE CELL

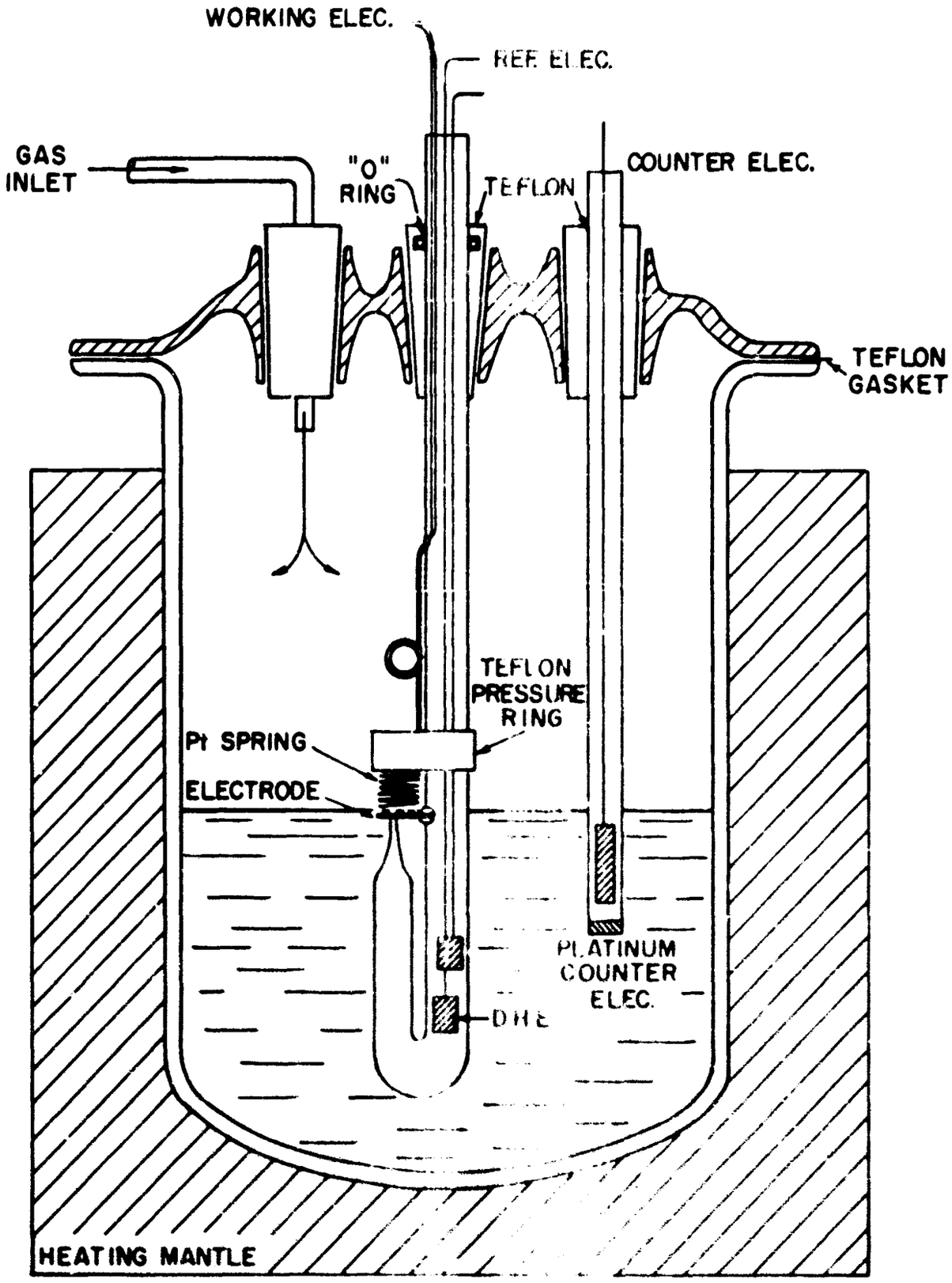

Fig. 1.2

downward pressure of a spring of Pt wire. The latter also acts as the conducting lead from the disc to the external circuit. A ring of Teflon which slides up and down the main support tube helps in keeping the Pt spring under compression and in firm position on the disc. Before each experiment the particular working electrode under test is positioned in the electrode holder and then introduced in the cell through the central opening in the cover. The relative dimensions of the electrode holder and the cell inlet as drawn in Fig. 1.26 are slightly out of proportion.

The reference electrode is a dynamic hydrogen electrode[57] (supported inside the main support tube), the potential of which differs only slightly from that of the reversible hydrogen electrode. This difference is found by calibration against a hydrogen-floating electrode at open circuit on each experiment and is of the order of - 30 mv. The Luggin capillary tip of the reference electrode is placed so that it is approximately 2 mm - about twice the external diameter of the capillary - from the surface of the pasted screen (working) electrode. This distance is fixed by the construction of the main support tube, thus making it unnecessary to measure the resistance correction for each new test.

The counter electrode is a foil of Pt (2 cm x 2 cm) which dips into a fritted cell compartment. The fine porosity frit essentially prevents any contamination of the bulk electrolyte by the electrolysis product formed at this counter electrode.

In all of the test experiments, the electrolyte is 85% phosphoric acid maintained at a constant temperature of 150 $\pm$ 1°C with a Matheson Lab-Stat. Before the fuel gas (propane) is fed into the cell container it is pre-saturated with water vapor in a 2 liter reaction kettle. The temperature of the water in this kettle is controlled at 93.3 $\pm$ 0.5°C using a Haake Circulator (Series "F"). The vapor pressure of water at this temperature gives a vapor pressure of water above phosphoric acid of 600 mm Hg which has been suggested as most convenient[54]. The pre-saturation is necessary in order to prevent the loss of water from the electrolyte.

Prior to an activity test the porous electrode sample to be tested is placed on the main support tube and then lowered into the cell container

through which N_2 is being passed. An "O" ring seal in the Teflon stopper maintains a gas tight seal while still allowing the height of the assembly to be adjusted. Visual observation is used to position the porous disc on the surface of the electrolyte. Experimentally, it has been noted that there is little effect on electrode polarization when the point of contact between disc and electrolyte surface is altered slightly. Thus it was found that raising or lowering the electrode by 3 mm from a position level with the electrolyte surface changed the current less than 2%, when using H_2 gas as fuel. When the electrodes are in position, the gas flow is switched from pre-saturated N_2 to pre-saturated fuel gas (propane). The electrochemical activity of the catalyst is then measured as outlined in the previous quarterly report.

The "steady state" i(E) curve is recorded using a Wenking potentiostat and a Greibach Model 500 dc milliammeter; the potential is monitored by a John Fluke Model 825A Differential dc voltmeter. A block design of the basic circuit is shown in Fig. 1.27.

The IR drop between the floating electrode and the tip of the Haber-Luggin capillary is determined using the interruptor technique, Fig. 1.28. A fast interruption is achieved using a C.P. Clare High Speed Mercury Relay. The initial potential drop immediately after current interruption is recorded on a Taktronix Type 561A oscilloscope (Fig. 1.29).

A method for continuous IR compensation[58] for the floating electrode has been built (Fig. 1.30). The current involves employing a Philbrick P25A operational amplifier as an isolated voltage inverter. A 0 - 1 Ω adjustable resistor is inserted in series with the counter electrode, the exact value to which it has to be adjusted is determined from the interruptor method of IR determination. The current flowing through the circuit causes a voltage drop equal to the IR potential. This potential is fed to the voltage inverter and back to the Wenking potentiostat to correct the potential input by an amount equal to the IR polarization. The adjustable set input potential to the Wenking potentiostat now becomes the true electrode potential and is the one monitored by the high impedance voltmeter.

A complete photograph of the "floating electrode" cell is shown in Fig. 1.31.

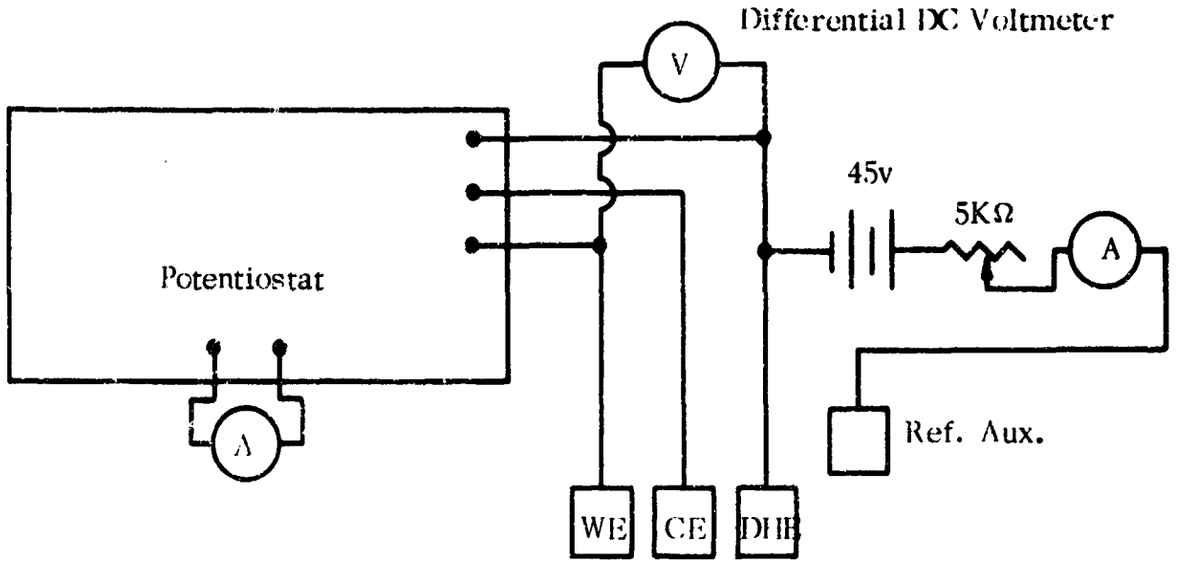

Fig. 1.27 Circuit diagram of potentiostatic arrangement for i(E) measurements on floating electrode.

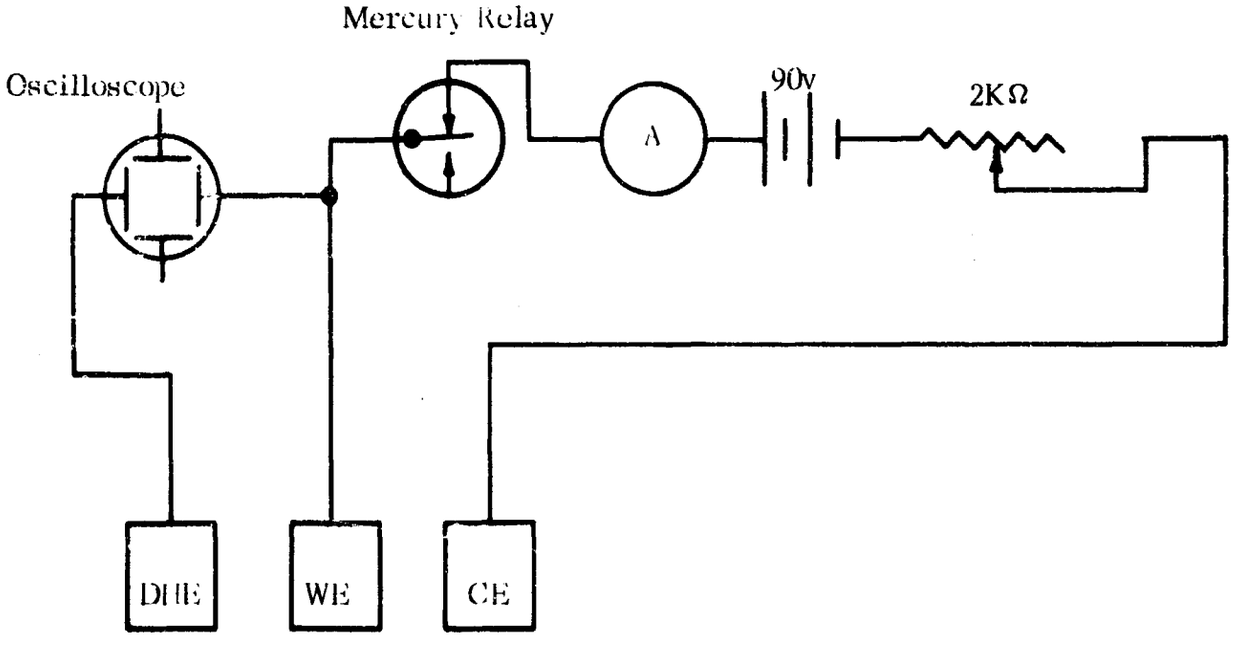

Fig. 1.28 Circuit diagram of interruptor with mercury relay.

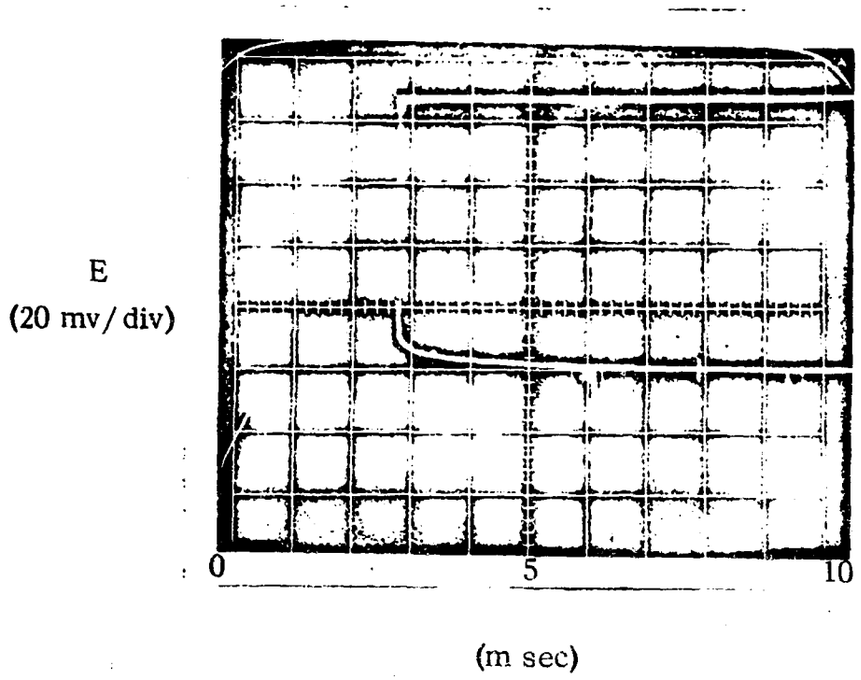

Fig. 1.29 Photograph of current interruption showing initial potential (IR) drop.

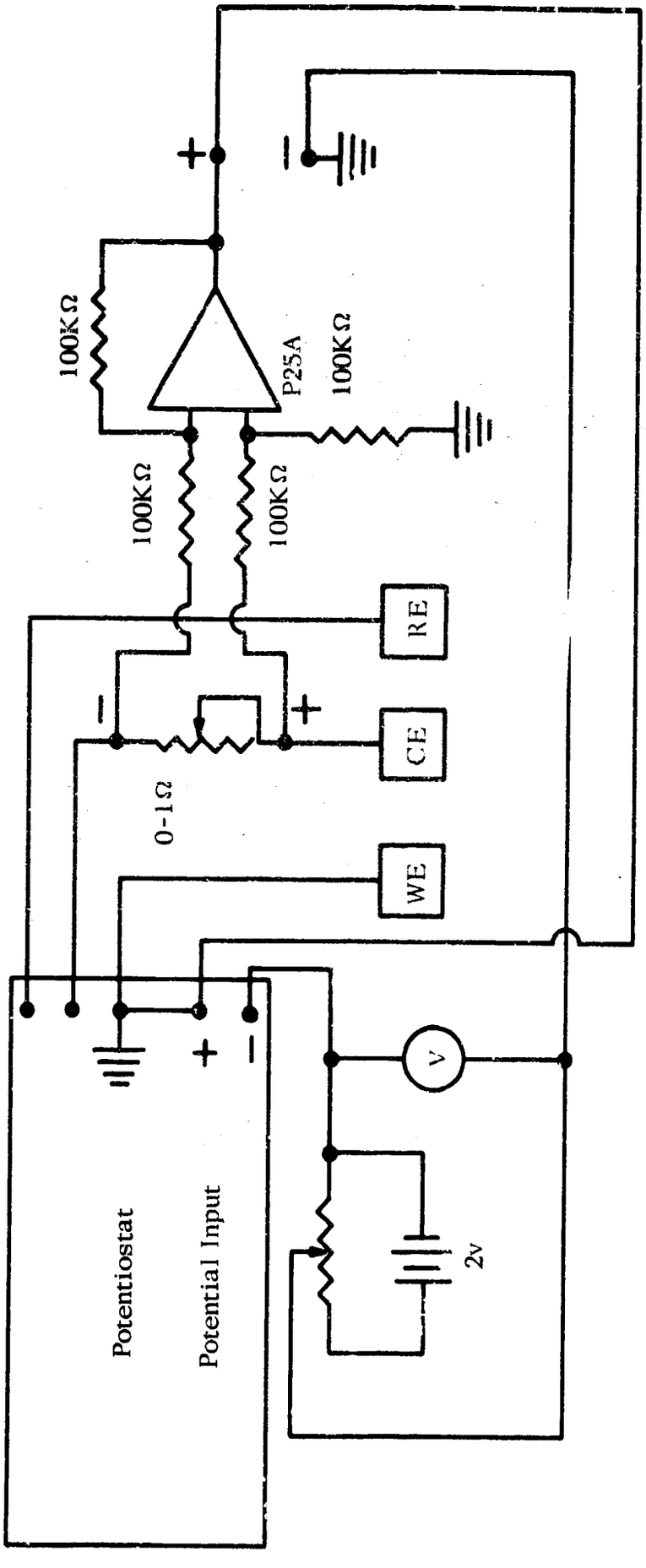

Fig. 1.30 Circuit diagram of IR compensator.

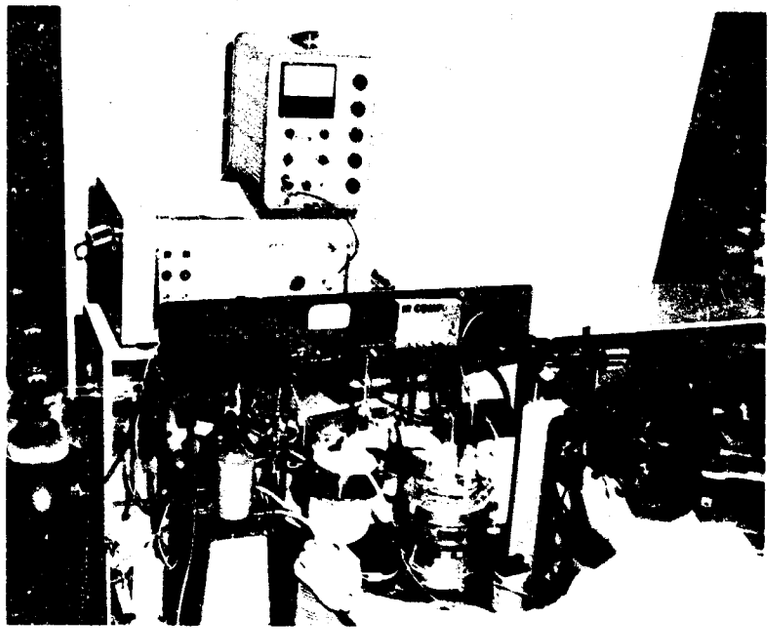

Fig. 1.31 Photograph of floating electrode assembly

2. Results. A number of preliminary experiments have been directed towards testing the apparatus and ascertaining that the technique of making electrodes (using platinum black supplied by Englehard Industries) gives activities comparable to commercially available electrode structures supplied by Cyanamid.

The results shown in Fig. 1.32 illustrate the similarity of the activities of the respective electrodes (with approximately the same Pt loading) and the good reproducibility of a number of electrodes prepared in the laboratory under identical conditions. Propane was used as fuel gas in all cases. Also from Fig. 1.32, it can be observed that the activity of the pasted electrodes increases with increase of the Pt black loading. This is as expected, but as yet we do not have enough results to decide upon the functional relationship between activity and Pt black loading.

The interpretation of results obtained using commercial preparations of Pt black in electrode structures and/or commercially prepared electrodes are strictly limited since the conditions under which the respective blacks are prepared, their characteristics, and the conditions under which commercial electrodes are bonded are not known.

3. Planned Experiments. Electrodes incorporating commercial platinum black are being constructed under different conditions (Pt black loading, sintering temperature, pressure); their activity will be measured using propane as fuel gas. Immediately after these measurements, the activity of electrodes incorporating selected platinum blacks that have been prepared in the laboratory (see above) will be measured. The activity (with respect to propane oxidation) of each sample will then be related to electrode construction factors (Pt black loading, sintering temperature, pressure), to preparation factors (reactant concentrations, temperature, induction time, etc.) and to the various characterization parameters, (surface area, average grain size and distribution, locked in stress, etc.).

Selected electrodes will also be subjected to fast potential sweep (~ 400 mv/min) measurements and to current decay measurements (with the potential set at say + 400 mv). These measurements will assist in further characterizing the electrochemical activity of the particular bonded Pt blacks.

Fig. 1.32

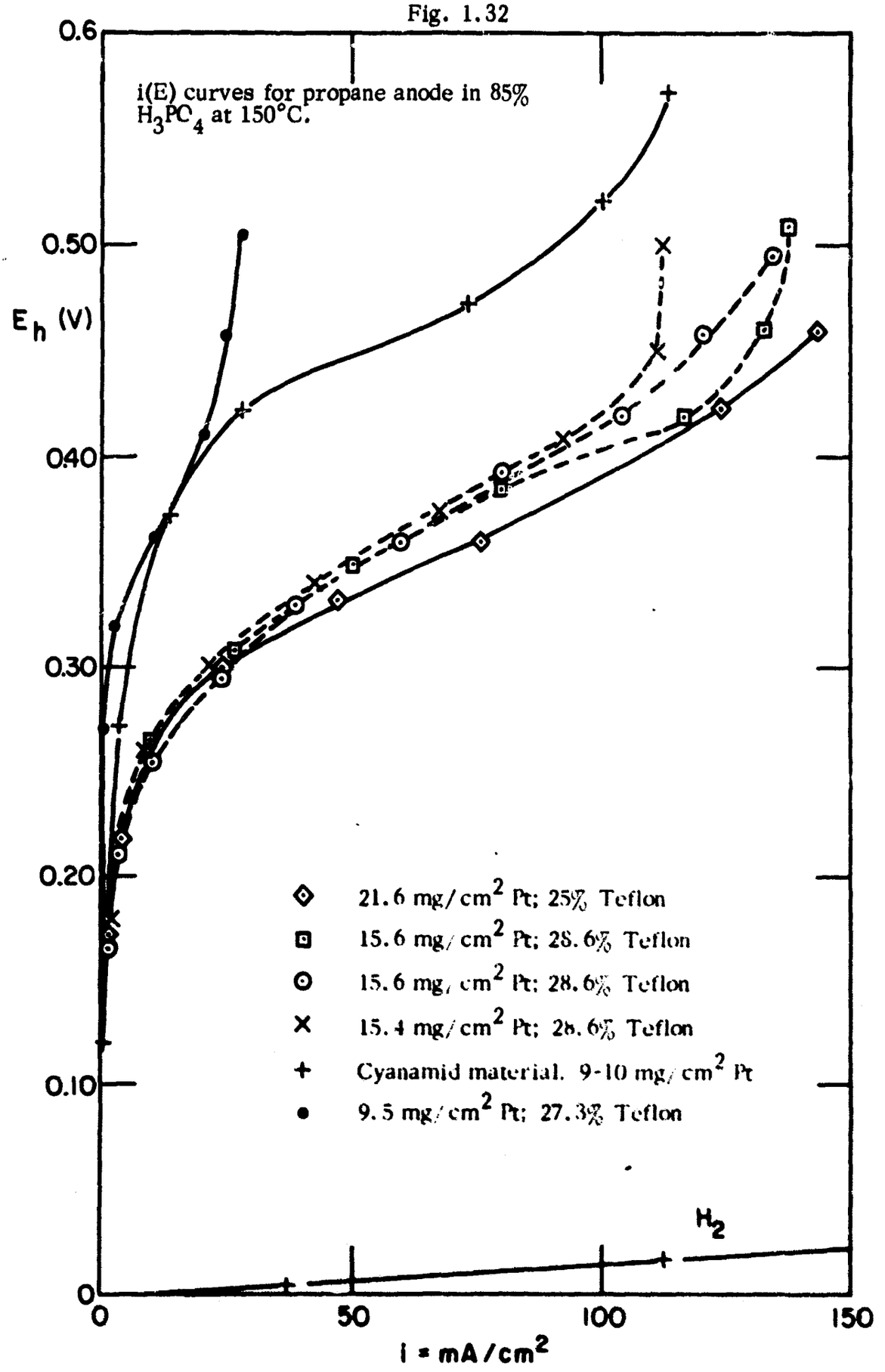
i(E) curves for propane anode in 85% H_3PO_4 at 150°C.
0.6
0.50
0.40
0.30
0.20
0.10
0
E_h (V)
21.6 mg/cm² Pt; 25% Teflon
15.6 mg/cm² Pt; 28.6% Teflon
15.6 mg/cm² Pt; 28.6% Teflon
15.4 mg/cm² Pt; 28.6% Teflon
Cyanamid material. 9-10 mg/cm² Pt
9.5 mg/cm² Pt; 27.3% Teflon
H_2
0
50
100
150
i = mA/cm²

```
C   FOURIER-STOKES METHOD FOR THE CORRECTION OF X-RAY DIFFRACTION
C   PEAKS FOR fi, PLATINUM BLACK, RELATIVE TO G, PLATINUM STANDARD.
C   INPUT DATA ARE IN TERMS OF TIME TO YIELD 2000 COUNTS.  OUTPUT
C   COEFFICIENTS ARE USED TO CALCULATE AVERAGE PARTICLE SIZE, TWINNING,
C   FAULTING, AVERAGE STRAIN AND STORED ENERGY.
    DIMENSION GR(9),GI(9),HR(9),HI(9),FR(9),FI(9),F(9),A(500),B(500),
     1G(500),H(500),FN(9)
    PI=3.14159
    3 FORMAT(6X,9F7.2)
   40FORMAT(81H    T      HR(T)      HI(T)      GR(T)      GI(T)      FR(T)      F
     1I(T)      F(T)      FN(T)    ///)
    5 FORMAT(1HO,F5.1,5F9.3,F8.3,F10.3,2F10.4)
    6 FORMAT(1H1)
  110 READ INPUT TAPE 5,111,K2
  111 FORMAT(I3)
  112 AN=K2-1
      READ INPUT TAPE 5,113,THETA
  113 FORMAT(F6.2)
   11 READ INPUT TAPE 5,3,(A(I),I=1,K2)
   12 READ INPUT TAPE 5,3,(B(I),I=1,K2)
  119 FORMAT(8X,I3,2(8X,F7.3)///)
  120 WRITE OUTPUT TAPE 6,6
  121 WRITE OUTPUT TAPE 6,122
  122 FORMAT(20X,45H-INTENSITIES OF PT STANDARD AND PT BLACK    )
  123 WRITE OUTPUT TAPE 6,124
  124 FORMAT(39H          I          G(I)          H(I))
  125 DO 129 I=1,K2
  126 G(I)=2000./A(I)
      H(I)=2000./B(I)
  128 WRITE OUTPUT TAPE 6,119,I,G(I),H(I)
  129 CONTINUE
   13 WRITE OUTPUT TAPE 6,6
   14 WRITE OUTPUT TAPE 6,4
   15 DO 42 N=1,9
   16 T=N-1
   17 GR(N)=0.0
   18 GI(N)=0.0
   19 HR(N)=0.0
   20 HI(N)=0.0
   21 DO 32 J=1,K2
   22 AJ=J-(K+1)/2
   23 ARG1=PI*AJ*T*2./AN
   24 GRP=G(J)*COSF(ARG1)/AN
   25 GR(N)=GR(N)+GRP
   26 GIP=G(J)*SINF(ARG1)/AN
   27 GI(N)=GI(N)+GIP
   28 HRP=H(J)*COSF(ARG1)/AN
   29 HR(N)=HR(N)+HRP
   30 HIP=H(J)*SINF(ARG1)/AN
   31 HI(N)=HI(N)+HIP
   32 CONTINUE
   33 DENOM=GR(N)*GR(N)+GI(N)*GI(N)
   34 FR(N)=(HR(N)*GR(N)+HI(N)*GI(N))/DENOM
      FI(N)=(HI(N)*GR(N)-HR(N)*GI(N))/DENOM
   35 F(N)=SQRTF(FR(N)*FR(N)+FI(N)*FI(N))
   37 FN=F(1)
   38 FN(N)=F(N)/FN
  300 WRITE OUTPUT TAPE 6,5,I,HR(N),HI(N),GR(N),GI(N),FR(N),FI(N),F(N),F
     1N(N)
   42 CONTINUE
```

```
 54 WRITE OUTPUT TAPE 6,6
    GYSUM=0.0
    GSUM=0.0
    THETA=0.0
    HYSUM=0.0
    HSUM=0.0
    HTHETA=0.0
    WRITE OUTPUT TAPE 6,7788
788 FORMAT(22H      CENTER OF GRAVITY   /)
    DO 2222 NJ=1,K2
    AG=NJ-1
    GTHETA=0.02*AG*G(NJ)
    GSUM=GSUM+GTHETA
    GYSUM=GYSUM+G(NJ)
    HTHETA=0.02*AG*H(NJ)
    HSUM=HSUM+HTHETA
    HYSUM=HYSUM+H(NJ)
222 CONTINUE
    CENTG=((GSUM/GYSUM)+THETA)/2.
    CENTH=((HSUM/HYSUM)+THETA)/2.
    WRITE OUTPUT TAPE 6,2444,CENTG,CENTH
444 FORMAT(10X,F8.6,10X,F8.6)
    CONTINUE
 79 GO TO 110
 80 END
```

VII. REFERENCES

1. B. D. Polkovonikov, A. A. Baladin and A. M. Taber, Dold, Akad. Nauk, SSSR 145, 809 (1962)
2. Fourth Interim Technical Report, Contract No. DA-009, AMC 410(T)
3. O. Loew, Ber. 23, 289 (1890)
4. R. Willstätter, and E. Waldschmidt Leitz, Ber. 54, 115 (1921)
5. R. Willstätter, and D. Hatt, Ber. 45, 1472 (1912)
6. B. Neuman, and E. Z. Goebel, Elektrochem. 39, 356 (1933)
7. A. Sieverts, and H. Brüning, Z. Anorg. Ch. 201, 113 (1931)
8. J. W. Döbereiner, Platin. p. 53 (Date and publisher unknown).
9. J. W. Döbereiner, Schw. J. 66, 299 (1832)
10. J. W. Döbereiner, Fogg. Ann. 28, 181 (1833)
11. J. H. Gladstone, and A. J. Tribe, J. Chem. Soc. 35, 175 (1879)
12. A. F. Benton, J. Am. Soc. 48, 1854 (1926)
13. L. Mond, W. Ramsay, and J. Shields, Phil. Trans. A186, 661 (1895)
14. L. Mond, W. Ramsay, and J. Shields, Z. phys. Ch. 19, 29 (1896)
15. A. Gutbier, and O. Maisch, Ber. 52, 1370 (1919)
16. F. Graf. Dissert. Jena (1926) 1927), p. 51
17. A.M. Wassiljew, Ucenye Zapiski Kazanskago Univ. [Russ] 90, 989 (1930)
18. A. Sieverts and H. Brüning, Z. Anorg. Ch. 201, 126 (1931)
19. H. Schulze, J. pr. Ch. [2] 32, 398 (1885)
20. J. W. Döbereiner, J. pr. Che. 1, 76 (1834)
21. J. W. Döbereiner, Platin. p. 65, 69 (Date and publisher unknown)
22. J. W. Döbereiner, Schw. J. 66, 299 (1832)

23. L. Wöhler, Ber. 36, 3481 (1903)

24. L. Wöhler, Habilitation-worle Karlsrude T. H. 1901, p. 39

25. R. Willstätter, and J. Jaquet. Ber. 51, 770 (1918)

26. L. Mond, W. Ramsay, and J. Shields, Phil. Trans. A190, 138, 141 (1897)

27. L. Mond, W. Ramsay, and J. Shields, Z. phys. Ch. 25, 667, 671 (1898)

28. H. Euler, Ofvers, Akad. Stockholm 1900, 271

29. A. W. McKee, J. Phys. Chem. 67, 841 (1963)

30. L. Wöhler, and C. Engler, Z. Anorg. Ch. 29, 5 (1902)

31. V. Voorhees, and R. Adams, J. Am. Soc. 44, 1397 (1922)

32. N. I. Kobosew, and W. L. Anochin, Z. phys. Ch. B13, 68 (1931)

33. M. W. Breiter and J. L. Weininger, J. Electrochem. Soc. 109, 1135 (1963)

34. A. Gutbier, and K. Neundlinger, Z. phys. Ch. 81, 209 (1913)

35. J. W. Döbereiner, Liev. Ann. 14, 15 (1835)

36. J. Giner, Electrochimica Acta. 8, 857 (1963), 9, 63 (1964)

37. S. B. Brummer and J. C. Makrides, J. Phys. Chem. 68, 1448 (1964)

38. W. Vielstick and U. Vogel, J. Electrochem. 68, 688 (1964)

39. J. Houben and A. Pfau, Ber. 49, 2295 (1916)

40. Ch. Courtot, Ann. Chim. [9] 5, 55 (1916)

41. R. Feulgen, Ber. 45, 360 (1921)

42. G. B. Taylor, G. B. Kistiakowsky, and J. H. Perry, J. Phys. Ch. 34, 748 (1930)

43. M. C. Boswell, and R. R. McLaughlin, Pr. Trans. Soc. Can. [3] 17, III 5 (1923)

44. B. E. Warren, Progress in Metal Physics, Pergamon Press, New York, 1959, p. 147

45. B. E. Warren and B. L. Averbach, J. Appl. Phys. 23, 1059 (1952)

46. A. R. Stokes, Proc. Phys. Soc. (London) 61, 382 (1948)

47. E. F. Bertaut, Acta Cryst. 3, 14 (1950)

48. K. Doi, Acta Cryst. 14, 830 (1961)

49. J. B. Cohen and C. N. J. Wagener, J. Appl. Phys. 33, 6, (1962)

50. Faulkner, Phil. Mag. 5, 519 (1960)

51. K. Doi and M. Mori, Jap. J. Appl. Phys. 3, 112 (1964)

52. L. W. Niedrach and H. R. Alford, J. Electrochem. Soc. 112, 117 (1965)

53. R. G. Haldeman, W. P. Colman, S. H. Langerand, W. A. Barber, Fuel Cell Systems, Advances in Chemistry Series No. 47, Amer. Chem. Soc. 106 (1965)

54. W. T. Griff and L. W. Niedra , J. Electrochem. Soc. 110, 1086 (1963)

55. J. Giner and S. Smith, J. Electrochem. Soc. Submitted for publication

56. Young, L., Anodic Oxide Films, Academic Press (1961)

57. J. Giner, J. Electrochem. Soc., 111, 377 (1964)

58. A. C. Makrides, J. Phys. Chem. 68, 2160 (1964)

PART 2

I. ABSTRACT

The corrosion of a number of metals, intermetallic compounds and alloys in hot, concentrated H_3PO_4 has been studied with the potentiostatic step technique. The metals Al, Ag, Co, Pb, Mo and Ni corrode very fast even at temperatures of only 80°C and cannot therefore be considered as possibilities for the major constituents of structural alloys. Cr corrodes slowly enough, even at 150°C, to show promise as an economically attractive alternative to Ta-based materials. However, thus far, intermetallic compounds based on Cr(e.g. Cr_2Ta, Cr_3Si, $CrSi_2$, Cr_3C_2) have been found to corrode more rapidly than Cr itself at elevated temperatures. The good corrosion resistance at elevated temperatures of a number of Ta compounds ($TaNi$, $TaNi_3$) and alloys (Ta - Ti) has been confirmed, but the resistance of other such compounds is surprisingly poor (e.g. $TaCo_3$). Possible reasons for this variation in behavior are discussed.

II. CORROSION IN H_3PO_4 SOLUTIONS

The practical development of the direct oxidation hydrocarbon fuel cell depends significantly on reducing the capital cost of its components. The difficulty is that hot concentrated H_3PO_4 is extremely corrosive: the only non-noble metal which has suitable corrosion resistance and also appropriate mechanical properties is pure Ta. In practice Ta is so expensive that it contributes as much to the total cost of the device as does the Pt catalyst.

The directions of the present work have been two-fold. On the one hand, we have sought to study some intermetallic compounds which have good corrosion resistance to the electrolyte and which we hope will give us an insight into the factors which determine corrosion resistance of the acid. On the other hand, we have investigated directly those metals and alloys which are inherently cheaper than Ta and should be structurally suitable. Although no non-noble metal other than Ta is known to have suitable corrosion resistance[1], we hoped in this way to uncover leads to promising, cheaper materials.

The experimental procedure is largely as described in our earlier report[1]. Samples were machined as cylinders of ~ 0.5 cm diameter and mounted in glass-tubes. Electrical contact was made with a spot-welded Pt wire and the electrode was sealed with shrinkable Teflon tubing. This arrangement was not always successful and we sometimes experienced leakage between the metal and Teflon. On some occasions, then, the electrode was just spot-welded to the Pt and the latter sealed through soft glass, with no effort being made to prevent electrolyte from contacting the Pt. In this event, no attempt can be made to work below the hydrogen reversible potential but this is in any case outside the potential region of the present interest.

Where the electrode material suffered thermal shock on spot-welding, a groove was machined in the sample; the Pt lead was fitted in this, and Pt was then twisted to make a firm contact with the sample. Current potential curves were usually taken point by point proceeding anodically from the open circuit potential. Two to ten min were spent at each potential, as was

appropriate for each sample. In some cases, to obtain reproducible results we reduced the surface oxides at a fixed potential before taking each point on the ascending potential regime. We feel that this is the most desirable way to obtain absolutely meaningful corrosion rates, but it is time consuming and we have employed it only where absolutely necessary. Measurements were taken from 80 to 150°C in 85% H_3PO_4.

The work with Ta intermetallic compounds and alloys described earlier has been continued and we have confirmed the superior corrosion resistance of $TaNi_3$ and Ta-Ti alloys. The corrosion of Ta-30 Ti (w % equivalent to about 65 a % Ti) in 85% H_3PO_4 is shown in Fig. 2.1. This material shows very good corrosion resistance, but at the highest temperatures, it is just not quite good enough to be considered as a possible structural material. Thus its corrosion rate at 150°C may be estimated as being about 6 mils per year, based on the 10 min-rate which is rather higher than the long term rate. This value is higher than the desired maximum rate of perhaps 4 mils per year for non-critical structural elements and < 0.1 mpy in electrode screens, etc. Also, we may note that at 65 a % Ti we still have 70 w % of Ta, and our major objective of eliminating the expensive element Ta cannot be achieved. It is not desirable to attempt to put any more Ti in Ta (even if the corrosion resistance were adequate) since segregation into two phases would occur at the temperatures of operation of the hydrocarbon fuel cell[2]. Despite these drawbacks we should not that the corrosion resistance of this alloy is really remarkable and is much better than that of Ti itself. For example at 1.0 V vs. R.H.E. at 80°C its corrosion rate is about 2 μ A/cm^2, whereas Ti dissolves at about 150 μ A/cm^2 (Fig. 2.7). This does suggest the possible value of alloying with relatively small amounts of Ta to confer corrosion resistance.

The corrosion of $TaNi_3$ and TaNi (5 min readings) is shown in Fig. 2.2. The corrosion rates of both $TaNi_3$ and TaNi at 150°C are small, that of the latter being better, as expected. Precisely what are the features (structural or atomistic) which confer such good resistance on these materials is not clear and investigations of each intermetallic

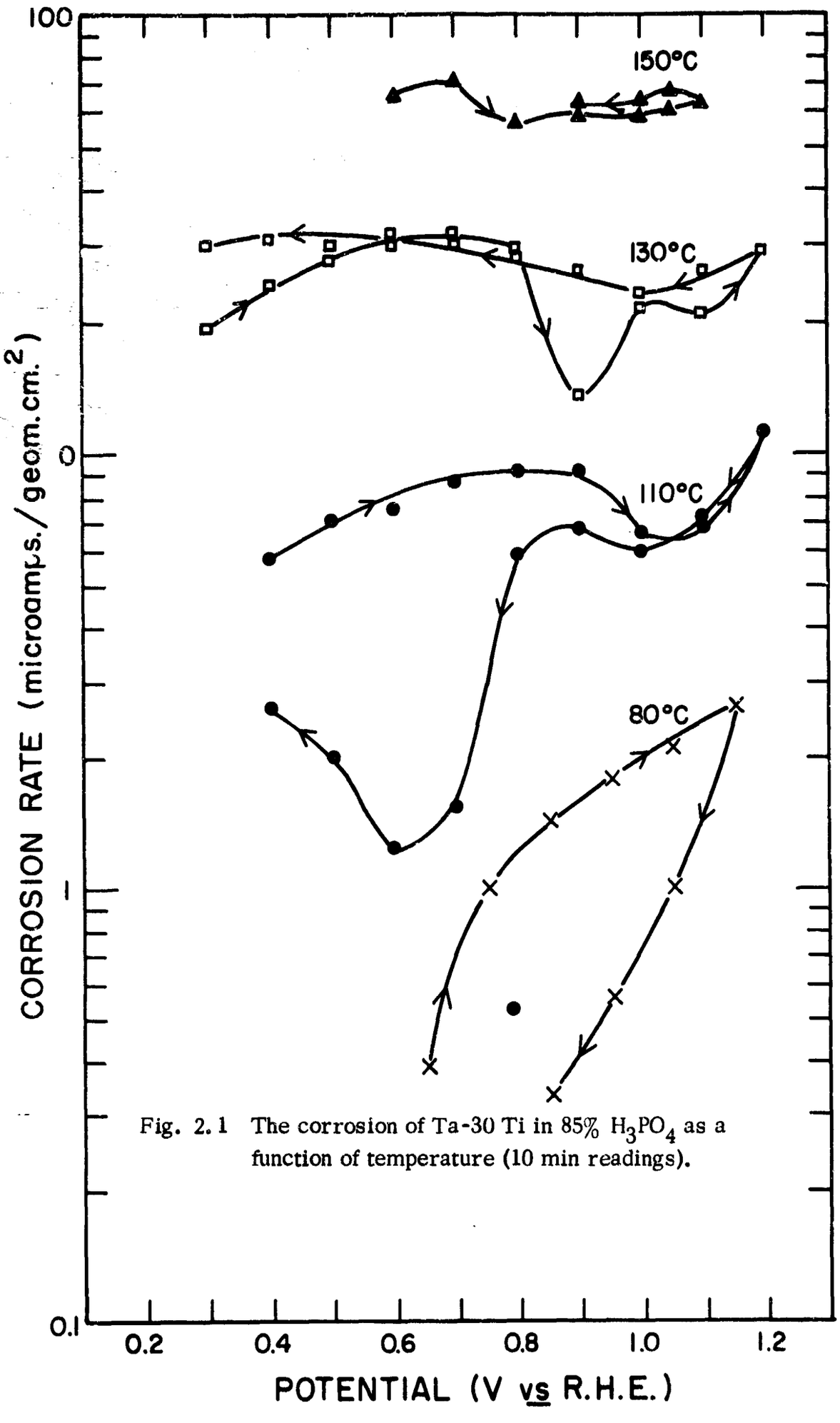

Fig. 2.1 The corrosion of Ta-30 Ti in 85% H_3PO_4 as a function of temperature (10 min readings).

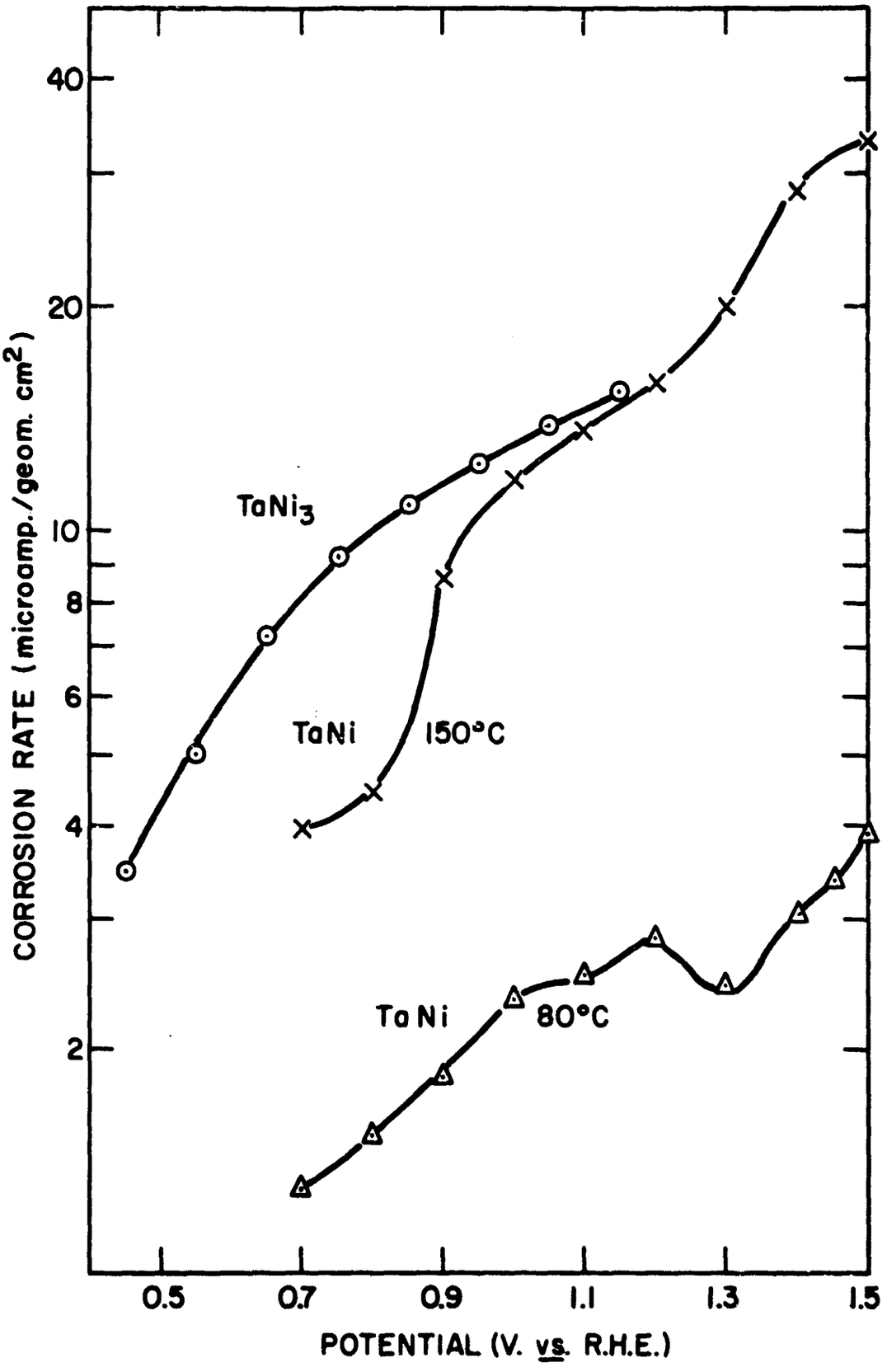

Fig. 2.2 The corrosion of $TaNi_3$ and TaNi in 85% H_3PO_4 (5 min readings).

compounds have been undertaken to pursue this question. We may note that although $TaNi_3$ has 75 a % Ni, it is still much more corrosion resistant than the parent element (Fig. 2.6).

Results for the corrosion of Co_3Ta and TiNi at 80°C are shown in Fig. 2.3. TiNi was selected because it is quite ductile which is particularly desirable here. It dissolves at about 300 μ A/cm^2, more or less independent of potential in the range 0.2 - 0.4 v vs. R.H.E., it is evidently in the passive region albeit the passive current is rather high. This corrosion rate contrasts with about 20 mA/cm^2 for Ni and about 200 μ A/cm^2 for Ti. Co_3Ta was chosen because, on general metallurgical grounds, it might be ductile and because from analogy with $TaNi_3$ it might well be corrosion resistant (Ni and Co are very similar in their resistance to the acid - Figs. 2.6 and 2.7). In any event, the corrosion resistance of the Co_3Ta is disappointing, being about 1.5 mA/cm^2 at 80°, only about 20 times less than Co itself (Fig. 2.7).

The poor corrosion resistance of the Co_3Ta compared to $TaNi_3$ is difficult to understand. From a purely thermodynamic viewpoint, $TaNi_3$ should be the more stable of the two compounds because it is congruently melting whereas Co_3Ta is not. This should not be relevant here, however, since the hysteresis which we find in the current-potential curves indicates that the materials are covered with oxide. Presumably in the case of $TaNi_3$ this oxide is essentially Ta_2O_5 whereas for Co_3Ta it is not. Yet from an ionic radius viewpoint, both Ni and Co ions should be able to substitute equally well for Ta^{+5} in the oxide, so they should both lead to stable oxide covers. Indeed, both Ni and Co do form tantalates (mixed oxides) with the same structure[3]. At this juncture, we assume that the reason for the large difference in corrosion resistance is some epitaxial mismatch between the Co_3Ta and the $CoTa_2O_6$ mixed oxide.

Another compound whose corrosion rate was much higher than expected from the behavior of the parent elements was $TaCr_2$ (Fig. 2.4). The corrosion-rate curve at 150°C resembles that of Ta[1] rather than that of Cr (Fig. 2.5) but is much higher. This rate is higher than that of Cr itself

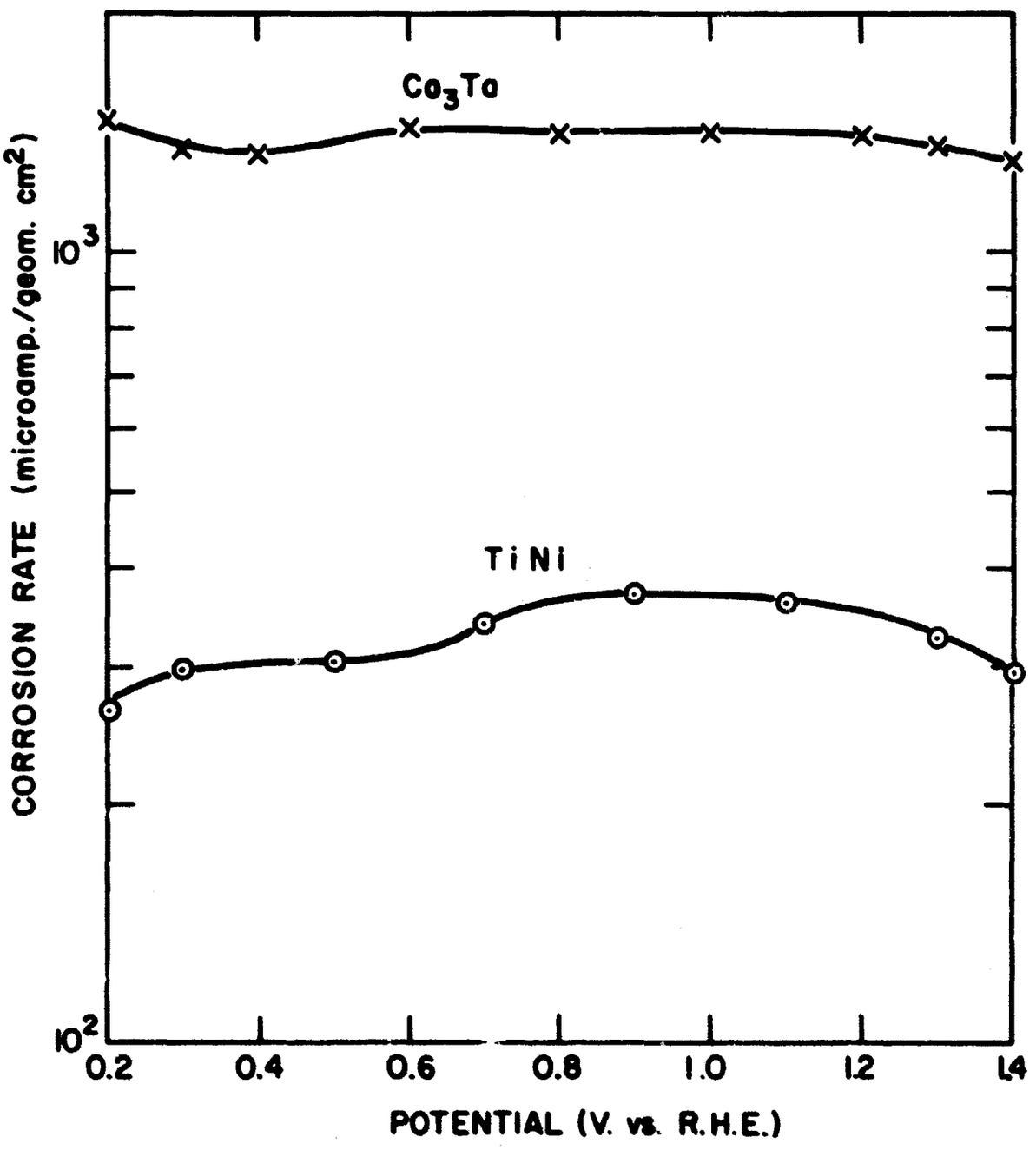

Fig. 2.3 The corrosion of Co_3Ta and TiNi in 85% H_3PO_4 at 80°C (2 min readings).

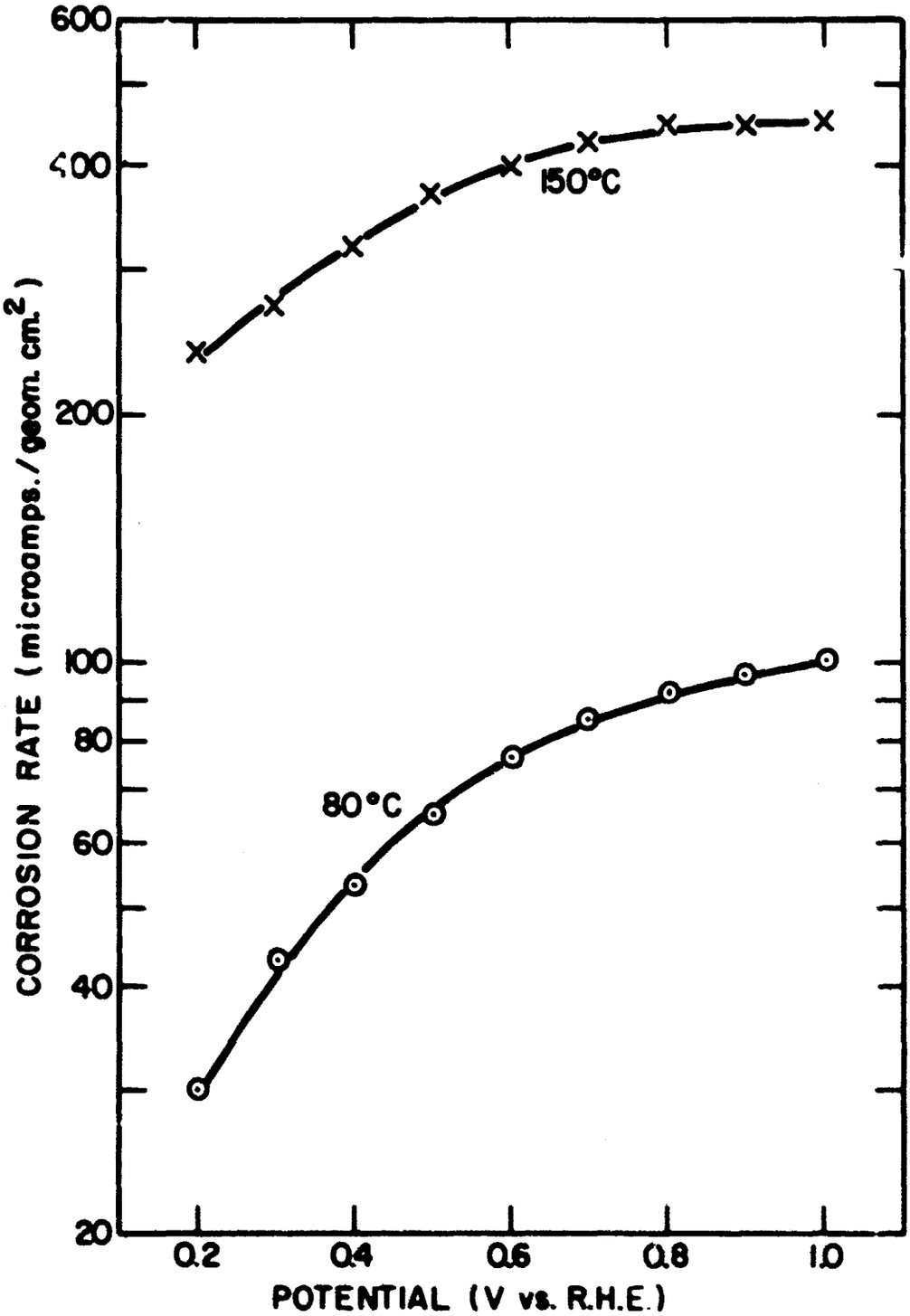

Fig. 2.4 The corrosion of $TaCr_2$ in 85% H_3PO_4 as a function of temperature (2 min readings).

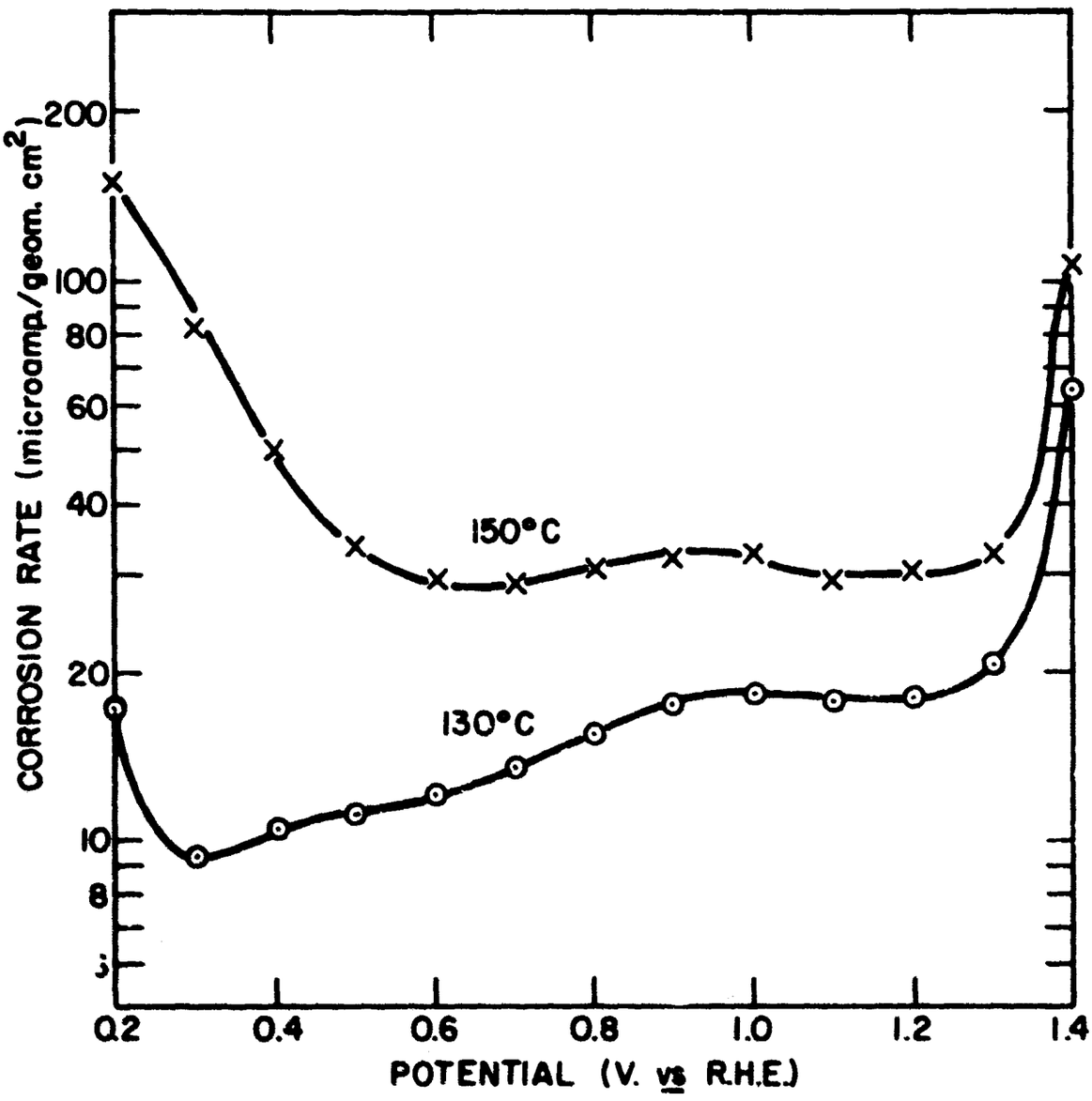

Fig. 2.5 The corrosion of Cr in 85% H_3PO_4 as a function of temperature (2 min readings).

(~ 30 μ A/cm^2), being about 450 μ A/cm^2 at 1.0 v at 150°C. This is a case where the corrosion rate of the compound is much worse than that of either of the combining elements.

A number of elements were tested for corrosion resistance in 85% H_3PO_4 in order to seek additional leads in the search for low cost Ta substitutes. The results are summarized in Figs. 2.5 - 7. Of these, only Cr showed any direct promise for the major component of a non-Ta containing alloy. The corrosion characteristic of Cr is however undesirable in a number of ways; for example, the rate at 150°C in the passive region (0.6 - 1.4 v) is equivalent to about 9 mils per year too much. Again, while the curve of Fig. 2.5 shows a typical active-passive transition, the metal is still active at the potential of the hydrocarbon anode. Therefore, alloying and/or compound formation to suppress the passive current and the active dissolution region are necessary to render the material useful. To this end, and following reports that the addition of Si confers useful acid resistance[4], we have investigated Cr-Si intermetallics. The results are shown in Fig. 2.8. Both Cr_3Si and $CrSi_2$ are more corrodible than Cr itself although there is some evidence that the active dissolution of Cr is suppressed by the addition of large amounts of Si. At 150°C the corrosion of Cr_3Si is at least 10 times worse than that of Cr itself. $CrSi_2$ corrodes about 10 times faster than Cr_3Si at 80°C. We have also investigated the corrosion of Cr_3C_2 (Fig. 2.9). Here, we find not only that the active dissolution of the Cr is unaffected but also that transpassive behavior sets in a low potentials (~ 0.8 v vs. R.H.E.). So far we have found that Cr intermetallic compounds are invariably worse than Cr itself even when combined with highly corrosion resisting elements.

It is as yet too early to draw general conclusions about corrosion resistance in H_3PO_4 from the relatively sparse data on intermetallic compounds. We may note that whereas in some cases (TaNi, $TaNi_3$) the passivating oxide (of Ta) is favored, in others (Cr_3Si, $CrSi_2$ and worst of all $TaCr_2$) the passivating oxide is destroyed and the corrosion is worse than expected. In most cases, the corrosion resistance of a compound seems to be intermediate between that of the elements. In some cases it is worse

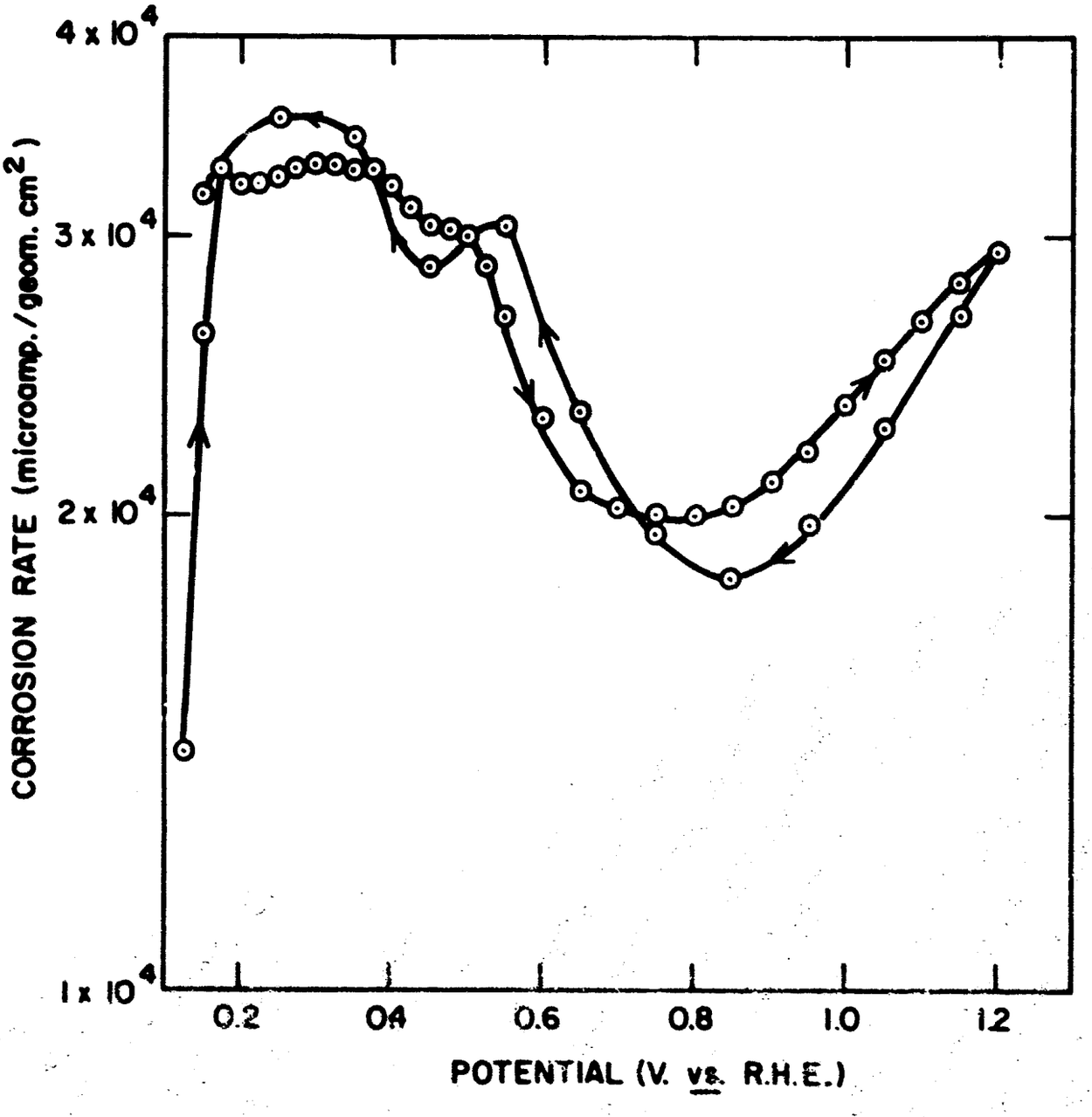

Fig. 2.6 The corrosion of Ni in 85% H_3PO_4 at 80°C (2 min readings).

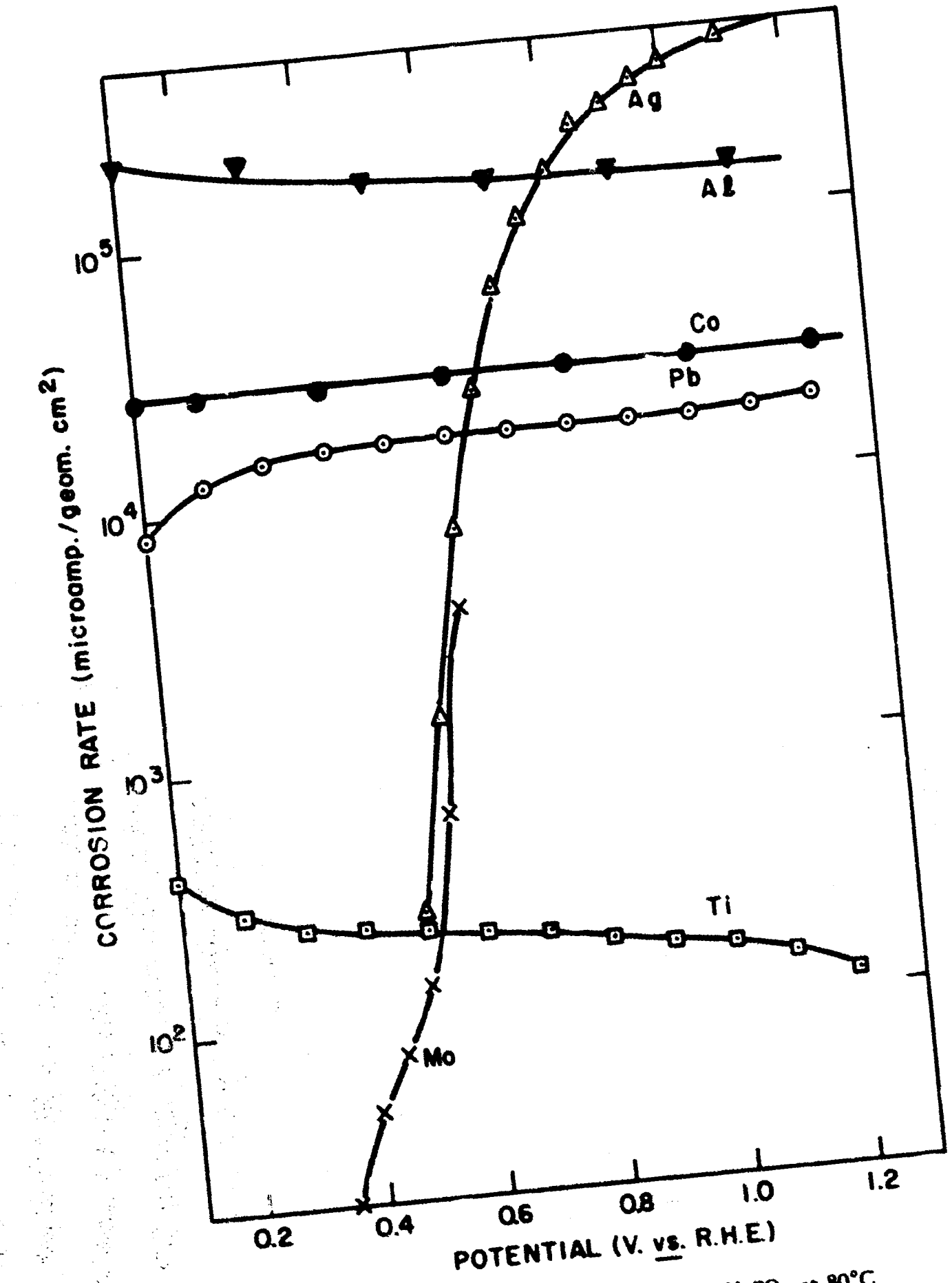

Fig. 2-7 The corrosion of various metals in 85% H_3PO_4 at 80°C (2 min readings).

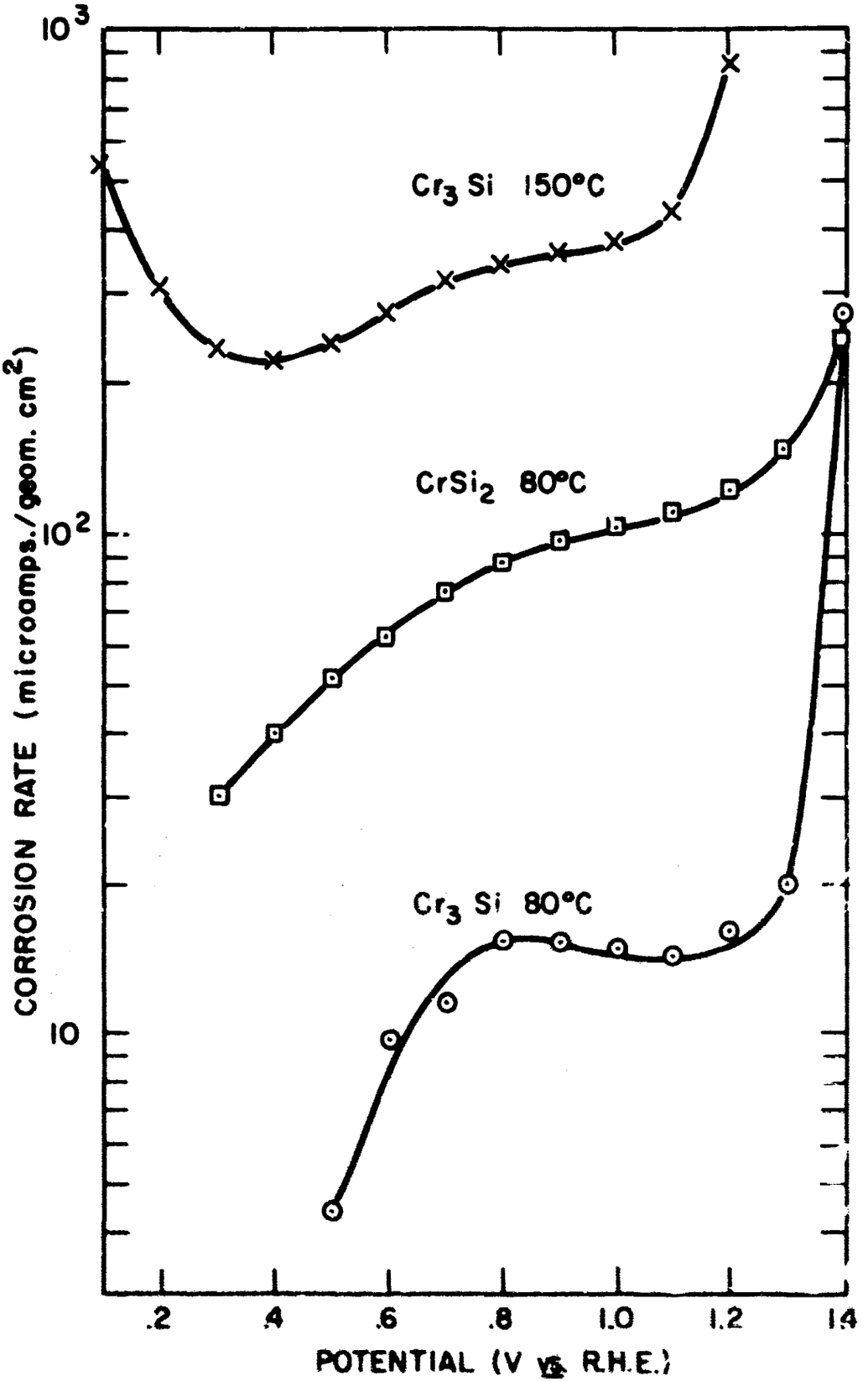

Fig. 2.8 The corrosion of Cr_3Si and $CrSi_2$ in 85% H_3PO_4 as a function of temperature (2 min readings).

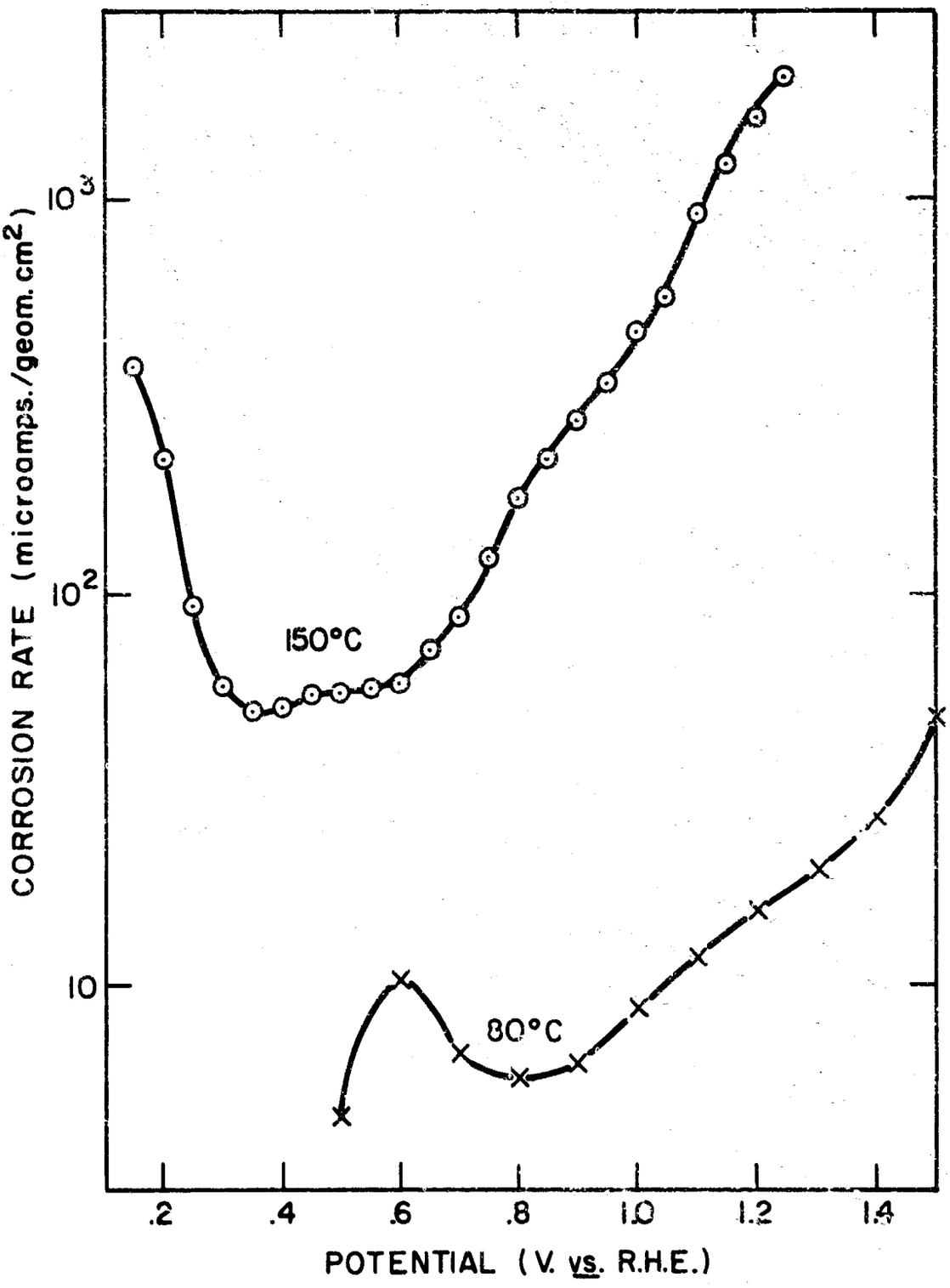

Fig. 2.9 The corrosion of Cr_3C_2 in 85% H_3PO_4 as a function of temperature (2 min readings).

than that of either element and so far we have not found a case where it is better than that of either element. The continuation of this line of approach would suggest the further investigation of families of intermetallic compounds with a view of elucidating those structural and chemical (atomic) features which make for good corrosion resistance.

III. REFERENCES

1. Fourth Interim Technical Report on this Contract, Nov. 1965
2. F. T. Sisco and E. Epremian, "Columbium and Tantalum," John Wiley, New York, N.Y. (1963)
3. A. F. Wells, "Structural Inorganic Chemistry," Oxford University Press (1962)
4. F. L. LaQue, and H. R. Copson, Corrosion Resistance of Metals and Alloys, Reinhold, New York, N. Y. (1963)